1985-03

Forecasting atmospheric visibility over the summer North Atlantic using the Principal Discriminant Method.

Elias, Kristine C.

Monterey, California. Naval Postgraduate School

NAVAL POSTGRADUATE SCHOOL
Monterey, California

THESIS

FORECASTING ATMOSPHERIC VISIBILITY OVER
THE SUMMER NORTH ATLANTIC USING THE
PRINCIPAL DISCRIMINANT METHOD

by

Kristine C. Elias

March 1985

Thesis Advisor: R. J. Renard

Approved for public release; distribution unlimited.

REPORT DOCUMENTATION PAGE		READ INSTRUCTIONS BEFORE COMPLETING FORM
1. REPORT NUMBER	2. GOVT ACCESSION NO.	3. RECIPIENT'S CATALOG NUMBER
4. TITLE (and Subtitle) Forecasting Atmospheric Visibility Over the Summer North Atlantic Using the Principal Discriminant Method		5. TYPE OF REPORT & PERIOD COVERED Master's Thesis March 1985
		6. PERFORMING ORG. REPORT NUMBER
7. AUTHOR(s) Kristine C. Elias		8. CONTRACT OR GRANT NUMBER(s)
9. PERFORMING ORGANIZATION NAME AND ADDRESS Naval Postgraduate School Monterey, CA 93943		10. PROGRAM ELEMENT, PROJECT, TASK AREA & WORK UNIT NUMBERS
11. CONTROLLING OFFICE NAME AND ADDRESS Naval Postgraduate School Monterey, CA, 93943		12. REPORT DATE March 1985
		13. NUMBER OF PAGES 112
14. MONITORING AGENCY NAME & ADDRESS (if different from Controlling Office)		15. SECURITY CLASS. (of this report) Unclassified
		15a. DECLASSIFICATION/DOWNGRADING SCHEDULE

16. DISTRIBUTION STATEMENT (of this Report)

Approved for public release; distribution unlimited.

17. DISTRIBUTION STATEMENT (of the abstract entered in Block 20, if different from Report)

18. SUPPLEMENTARY NOTES

19. KEY WORDS (Continue on reverse side if necessary and identify by block number)

Model Output Statistics
Visibility
North Atlantic Ocean Visibility
Marine Visibility
Visibility Forecasting
Principal Discriminant Method
Categorical Forecasting
Ocean Areas
Homogeneous Ocean Areas

20. ABSTRACT (Continue on reverse side if necessary and identify by block number)

This report describes the application and evaluation of the Principal Discriminant Method (PDM) in the forecasting of horizontal visibility over selected physically homogeneous areas of the North Atlantic Ocean. The main focus of this study is to propose a possible model output statistics (MOS) approach to operationally forecast visibility at the 00-hour model initialization time and the

#20 - ABSTRACT - (CONTINUED)

24-hour and 48-hour model forecast projections, using as data the period 15 May--7 July 1983. The technique utilized involves the manipulation of observed visibility and the Fleet Numerical Oceanography Center's Navy Operational Global Atmospheric Prediction System (NOGAPS) model output parameters. Both two-and three-category visibility models were examined. The resulting zero-and one-class errors as well as the threat scores from the PDM model were compared with those obtained from maximum probability and natural regression studies. For the majority of the experiments performed, PDM was outperformed by the other techniques, although one trial run of an adjusted PDM technique gave results very similar to those of the maximum probability techniques.

Approved for public release; distribution unlimited

Forecasting Atmospheric Visibility Over the Summer North Atlantic Using the Principal Discriminant Method

by

Kristine C. Elias
Lieutenant Commander, United States Navy
A.B., University of California, Riverside, 1973

Submitted in partial fulfillment of the
requirements for the degree of

MASTER OF SCIENCE IN METEOROLOGY AND OCEANOGRAPHY

from the

NAVAL POSTGRADUATE SCHOOL
March 1985

ABSTRACT

This report describes the application and evaluation of the Principal Discriminant Method (PDM) in the forecasting of horizontal visibility over selected physically homogeneous areas of the North Atlantic Ocean. The main focus of this study is to propose a possible model output statistics (MOS) approach to operationally forecast visibility at the 00-hour model initialization time and the 24-hour and 48-hour model forecast projections, using as data the period 15 May--7 July 1983. The technique utilized involves the manipulation of observed visibility and the Fleet Numerical Oceanography Center's Navy Operational Global Atmospheric Prediction System (NOGAPS) model output parameters. Both two-and three-category visibility models were examined. The resulting zero-and one-class errors as well as the threat scores from the PDM model were compared with those obtained from maximum probability and natural regression studies. For the majority of the experiments performed, PDM was outperformed by the other techniques, although one trial run of an adjusted PDM technique gave results very similar to those of the maximum probability techniques.

TABLE OF CONTENTS

LIST OF TABLES

LIST OF FIGURES

I. INTRODUCTION AND BACKGROUND

The Model Output Statistics (MOS) technique involves the processing of atmospheric parameters output from numerical weather prediction models (predictors), along with observed data, to produce forecast algorithms of meteorological parameters (predictands). The predictands are either operationally important parameters not forecast by numerical models (e.g.,visibility, cloud amount, ceiling) or model output parameters whose predictive skills are improved (e.g.,surface wind, temperature) due to partial correction of numerical model bias and/or scale.

The National Weather Service (NWS) uses a linear, least-squares regression model to generate empirical forecast equations. This MOS technique has demonstrated operationally usable skill in forecasting numerous weather elements at land locations throughout the world [Best and Pryor, 1983]. Both the United States Air Force and Navy have made limited use of the NWS model for selected land areas around the world. The Navy has attempted to forecast open-ocean fog and visibility using linear regression equations, with the resultant skill levels exceeding persistence, climatology and those of the NWS as well. However, these limited experiments produced results considered only marginally useful for operational situations

[Aldinger,1979; Yavorsky, 1980; Selsor, 1980; Koziara, et al, 1983; Renard and Thompson, 1984]. Undoubtedly, this performance level is due, in part, to the lack of 'calibrated' fog and visibility observations. At sea, weather observers lack the reference points necessary to accurately estimate the visibility.

Because of the potential for success demonstrated by the above cited experiments, the Navy began development of an MOS program in the spring of 1983 to forecast operationally important air/ocean parameters over all ocean areas in both hemispheres. Horizontal visibility was selected as the first parameter to be investigated due to its importance to the mariner. Because linear regression techniques over land areas (NWS, 1960--date) and the North Pacific Ocean (Navy, late 1970's) demonstrated considerably less-than-perfect results, other statistical methods were proposed to determine if a better one could be found.

Preisendorfer (1983 a,b,c) proposed three strategies, two based on maximum probability and one based on natural regression. Lowe (1984a) proposed innovative threshold techniques to be applied with the linear regression approach. All of these methods were developed, applied and tested on North Pacific and North Atlantic Ocean areas by Karl (1984) and on additional North Atlantic Ocean areas by Diunizio (1984a) in their investigations of visibility.

Wooster (1984) applied the same techniques to cloud amount and ceiling height parameters.

This study presents a Principal Discriminant Method (PDM) of statistical analysis as developed for the MOS problem by Preisendorfer (1984). Significance testing methods proposed by Mr. Paul Lowe, Naval Environmental Prediction Research Facility,[*] and investigated by Diunizio (1984b), were also utilized. These results are compared with results obtained from the aforementioned methodologies.

In the following discussion, a sufficient number of terms and symbols are defined to allow readers without strong statistical backgrounds to understand the results. However, for a proper understanding of the Preisendorfer (1984) methodology, readers are encouraged to examine Appendix A for a detailed discussion. Details on the significance testing [Diunizio, 1984b] are found in Appendix B.

---

[*]Conversation, and unpublished notes.

II. OBJECTIVES AND APPROACH

The objective of this study is to determine if the Principal Discriminant Method (PDM), applied to discrete values of model output and derived parameters, can improve upon the forecasting of horizontal marine atmospheric visibility when compared to the Preisendorfer natural regression and maximum probability approaches. The PDM approach is outlined as follows:

a. define visibility groups, categorized in a way which relates most closely to operational use at sea.

b. develop and apply the Preisendorfer (1984) PDM to three North Atlantic Ocean physically homogeneous areas [Lowe, 1984b], using 15 May through 7 July 1983 Navy Operational Global Atmospheric Prediction System (NOGAPS) predictor data.

c. compare and contrast the individual results with those Preisendorfer statistical methodologies previously explored by Karl (1984) and Diunizio (1984a).

d. Based on a. to c. above, present an interim recommendation for an optimal statistical approach to forecasting horizontal visibility in the North Atlantic Ocean as a function of prediction time and homogeneous area.

III. DATA

A. VISIBILITY OBSERVATIONS AND SYNOPTIC CODE

Horizontal visibility observations taken from seagoing platforms are reported as values of ten standardized World Meteorological Organization (WMO) synoptic weather codes (Appendix C). These codes range in value from 90, which corresponds to visibility less than 50 m, to 99, which corresponds to visibility equal to or greater than 50 km. Human observational error and inexactness in measuring visibility at sea necessitate a reduction of visibility classification categories for prediction purposes.

1. Three-Category Case

Initially, a three visibility category classification scheme was considered.

Visibility Category	Synoptic Code	Visibility Range
I	90-94	<2 km
II	95-96	≥ 2 km to <10 km
III	97-99	≥ 10 km

The above scheme is the same as that used by Karl (1984) and Diunizio (1984a); it is based upon the following at-sea operational criteria followed by the U. S. Navy.

1. 10 km (5 n mi)--U.S. Navy aircraft carrier at-sea flight recovery operations change from visual (VFR) to controlled (IFR) approach guidelines [Department of the Navy, 1979].

2. 2 km (1 n mi)--the sounding of reduced visibility signals for all vessels operating in international waters. The term "reduced visibility" is not specifically defined in the International Regulations for Preventing Collisions at Sea, 1972. The distance of 1 n mi is generally considered to be the governing operational distance.

2. Two-Category Case

In the past [Renard and Thompson, 1984], forecasting skill for category II has proved to be minimal. In the preliminary work for this study, it was noted that the predictor means of all three category subsets, as a function of associated predictand values, were not always well separated. Without good separation, a good statistical forecast is not possible regardless of the method used. It was noted however, that even though not all three means were well separated, at least two of the means were well separated from each other. This finding suggested that a two-category case might be better supported by the data. If the two-category case showed better data support than the three-category case, then enhanced results might be expected. To test this hypothesis, two different two-category data sets were created for experimentation. The two cases are:

Case X

Visibility Category	Synoptic Code	Visibility Range
IX	90-95	<4 km
IIX	96-99	≥ 4 km

Case Y

Visibility Category	Synoptic Code	Visibility Range
IY	90-94	<2 km
IIY	95-99	≥2 km

B. NORTH ATLANTIC OCEAN DATA

1. Area

The North Atlantic Ocean, from 0° to 80° N latitude, was divided into homogeneous oceanic areas by Lowe (1984b), using a statistical cluster analysis technique. The homogeneous areas evaluated in this study are identified as areas 2, 3W and 4 which represent areas of moderate, frequent and sparse occurrences of poor visibility, respectively (Fig. 1).

2. Time Period

Data from mid-May 1983 to mid-July 1983 were combined to form a more extensive data set, hereafter referred to as FATJUNE 1983.* The FATJUNE period was selected as the initial data set for statistical experimentation because of the climatologically high frequency of occurrence of poor visibility observations for many areas of the North Atlantic Ocean during this period. Only the 1200 GMT synoptic ship report data, corresponding

*However, NOGAPS predictor data for the period 15 May--7 July 1983 only were available for the study.

to daylight conditions, were used in this preliminary study of the method.

For the purpose of this study, TAU-00 generally represents six-hour model forecast fields. However, temperature, geopotential height and wind are model initialization fields. TAU-24 and TAU-48 are defined as 24-h and 48-h model forecast fields. All of the above are valid at 1200GMT. TAU-00, TAU-24 and TAU-48 model output parameters (predictors) are employed in the 00-h, 24-h and 48-h forecast schemes, respectively. Summaries of the number of observations in each visibility category of the dependent and independent data sets, as a function of homogeneous area and prediction time for FATJUNE 1983, are contained in Tables I-IV.

3. Synoptic Weather Reports

All synoptic visibility observations (predictand data) for this study were provided by the Naval Oceanography Command Detachment (NOCD), Asheville, North Carolina which is co-located with the National Climatic Data Center (NCDC). The observations which contained systematic observer error or were obviously erroneous, as determined from the data quality indicators provided with the data, were deleted from the working data sets.

4. Predictor Parameters

Fifty TAU-00, fifty-four TAU-24 and fifty-four TAU-48 model output predictors (MOP's) were provided by the

Fleet Numerical Oceanography Center (FNOC), Monterey, California. The parameters are generated by their current operational atmospheric prediction model, NOGAPS. All MOP's were interpolated from model grid coordinates to synoptic ship report positions using a linear interpolation scheme. In addition to the initial group of MOP's, thirteen derived parameters representing calculated quantities, such as parameter gradients and products, were included as potential predictors. Of the available predictor parameters, fifteen were eliminated from consideration because 1) the MOP lacked a physical linkage to the visibility predictand, and/or 2) a lack of significant digits (lost during the transfer of the FNOC data to the main computer center mass storage system) rendered the particular MOP useless. A list of all TAU-00, TAU-24 and TAU-48 MOP's available to the experiments are included in Appendix E.

C. DATA SETS

1. Standarization

NOGAPS analysis/forecast parameters are output in a large variety of units/scales. To eliminate the effect of different units of the various predictors on the Principal Discriminant Method (particularly the part using principal component analysis), the data were standardized before the method was applied. Given $x_1, \ldots, x_n$ members in each predictor group, the standardized members $y_1, \ldots, y_n$ are

given by

$$y_j = \frac{x_j - \bar{x}}{s}$$

where

$$\bar{x} = \frac{1}{n}\sum_{j=1}^{n} x_j, \text{ the mean}$$

$$s = \left[\frac{1}{n-1}\sum_{j=1}^{n}(x_j - \bar{x})^2\right]^{\frac{1}{2}}$$, the unbiased estimate of the standard deviation.

In this way all units were removed, the data centered at 0, and the variance of each of the data sets became 1.

2. <u>Dependent/Independent Data Sets</u>

Since FATJUNE 1983 was the only data set available for this study, the data were divided into two groups. Approximately two-thirds of the data became the dependent set upon which the model was based. This set is also referred to as the <u>training set</u>. The remaining one-third of the data became the independent set on which the model was tested. This set is also referred to as the <u>testing set</u>.

To insure that no biases existed in the sets, each training-testing set pair was created by use of a uniform random number generator. The given data sets were randomly split and then checked to insure they represented the initial population mean within a 95% confidence interval. Once created, these sets were used consistently throughout all model runs.

IV. PROCEDURES

A. TERMS AND SYMBOLS

The following terms and symbols are used throughout the remainder of this thesis and are briefly defined here to assist the reader. For more definitive mathematical expressions of potential errors, consult Appendix A. Mathematical expressions for class errors, threat scores and adjusted class errors may be found in Appendix D.

1. A0--the estimated probability (based on actual predictions using the testing set) of a zero-class visibility category forecast error (e.g., if visibility category I is forecast, it is also observed).

2. A1--the estimated probability (based on actual predictions using the testing set) of a one-class visibility category forecast error (e.g., if visibility category I is forecast and category II is observed).

3. A2--the estimated probability (based on actual predictions using the testing set) of a two-class visibility category forecast error (e.g., if visibility category I is forecast and category III is observed).

4. PA0--the estimated probability (based on the training set) of a zero-class visibility category forecast error.

5. PA1--the estimated probability (based on the training set) of a one-class visibility category error. (PA2 is defined similarly.)

6. Potential skill scores--(PA0,PA1 above) may be interpreted as follows. Randomly partition a data set (such as FATJUNE 1983) many times into training-testing set pairs. Fit probability distributions to the category subsets of the

training set as described in PDM. Then produce PA0, PA1 values (using the training set) and actual A0, A1 values (using the testing set). Repeat this for all the training-testing set pairs. Take the average of all PA0 values and all A0 values. In the limit of a sufficiently large number of partitions of the data set, these averages will tend to agree. Similarly for PA1, A1, and PA2, A2.

7. Correlation coefficient--a numerical measure of the relationship between one predictor and another. The value of the correlation coefficient ranges from -1 for negative correlation to +1 for positive correlation. The larger the absolute value of the correlation coefficient, the more closely are the predictors correlated.

8. P-value--the result of a two-sided significance test on separate variance t-test statistics. This gives a measure of the separation of the data into different visibility categories.

9. TS1--threat score for visibility category I computed from a contingency table.

10. Maximum probability strategy--choosing forecast visibility category based upon the highest conditional probability of the predictand categories for a given a predictor interval.

    a. MAXPROB I--designation of a maximum probability strategy in which ties of the highest conditional probabilities in a predictor interval are resolved by the generation of a random number

    b. MAXPROB II--designation of a maximum probability strategy in which ties of the highest conditional probabilities for a given predictor interval are resolved by assigning the lowest visibility category, of those ties, as the forecast category.

11. Natural regression strategy--choosing forecast visibility categories based upon the statistical average of the conditional probabilities of visibility for a given predictor interval.

12. Functional dependence. This is a measure of the stochastic dependence of one predictor upon another. Functional dependence is an estimate of the probability that one of the predictors will change

when the other changes. High functional dependence values between one already selected predictor and another potential predictor indicates that little additional information beyond the selected predictor is possible. The specific derivation and mathematical description of the concept of "functional dependence" is discussed in greater depth by Preisendorfer (1983c).

13. Root-sum-squared functional dependence. The functional dependence of a predictor on all predictors already included in the developmental model. It is equal to the square-root of the sum of the squares of the individual functional dependence values.

14. AAO--adjusted AO. A contingency table statistic which removes the influence of the most frequent visibility category in a set of data (similar to a normalized value).

15. CE--class error parameter defined as AO + 2A1 used as the primary aid in identifying the first predictor in the Preisendorfer (1983a,b,c) PR models.

16. PP--the potential predictability of visibility by any given predictor.

B. COMPUTER PROGRAMS

Four computer programs were developed to test the proposed Preisendorfer (1984) Principal Discriminant Method (PDM) methodology. The programs are on file in the Department of Meteorology, Naval Postgraduate School, Monterey, California 93943.

1. A program to standardize the data and create training and testing sets for homogeneous areas, depending on whether the two-or three-category strategy was in use.

2. A program to compute correlation coefficients between chosen and unchosen predictors, sorting them from low to high values.

3. A program to compute PA0, PA1, A0 and A1 values for each predictor and to check the PA0 values for significance against chance.

4. A program to compute PA0, PA1, A0 and A1 values for two or more predictors using binary decomposition. This program also computes contingency tables and threat scores.

C. PREISENDORFER PDM METHODOLOGY

1. <u>Determination of the First Predictor</u>

Selecting the first predictor is a two-step process. The first step involves computing the initial statistics (PA0, PA1) for each predictor. Secondly, based on output from BMDP Statistical Software program P7D [University of California, 1983],the average P-value for each predictor is computed and these values are ranked from low to high. The low values indicate better separability of the category populations. Therefore, the first predictor chosen is the one with the smallest averaged P-value. If more than one predictor shares the same low P-value, then of those predictors, the one with the highest PA0 value is selected as the first predictor.

2. <u>Choosing the Second and Subsequent Predictors</u>

The prospective second predictor in the model is determined from its correlation coefficient with the already chosen first predictor. The prospective second predictor has the smallest absolute value of the correlation coefficient. Whether it will ultimately be chosen as the second predictor depends on the following:

a. PA0 has increased, and

b. PA1 has decreased or remained constant, and

c. the averaged P-value is significant, i.e., less than .05.

If the prospective predictor cannot meet these criteria, then the next least correlated predictor is tried until all predictors have been exhausted.

This process is repeated for the multi-predictor stage until the model is complete.

3. Terminating the Selection of Predictors

Model development continues until <u>any one</u> of the following four conditions is met:

a. no more predictors remain to be considered, or

b. PA0 and/or P-scores are no longer significant with respect to the null hypothesis, or

c. criteria required to add additional predictors cannot be met.

Once the model development is complete, actual zero-and one-class errors (A0,A1) are computed using the independent data set. The resulting PA0, PA1, A0 and A1 values provide the measurement statistics on which the usefulness of the model is based.

D. PREISENDORFER (PR) MODEL

This model represents the application of the Preisendorfer (1983a,b,c) methodology (PR) explored by Karl (1984) and Diunizio (1984a). Karl's study provides specific details on the method and readers interested in a

more thorough presentation may consult it. This discussion is presented as a prelude to comparing results of the PR model to the Preisendorfer (1984) PDM model of this study.

As with the PDM model, the PR model utilizes NOGAPS model output and derived parameters as potential predictors in constructing a developmental model, based upon the dependent training data set, which provides the structure by which the model is tested and evaluated. (However, as applied by Karl and Diunizio, the data sets were not formed randomly nor were the means of the sets constrained to be representative of the entire population from which they were drawn. Instead, the visibility category groups were constrained to show similar percentages, for both the independent and dependent data sets.) The range of values of these predictors is partitioned into discretized equally populous predictor intervals ("cells") and conditional probabilities of the predictand are calculated according to the three previously defined VISCAT's. There are three separate strategies for determining the VISCAT to be identified with each predictor value. These strategies are MAXPROB I and MAXPROB II based on maximum probability, and a natural regression approach.

The sizes of the equally populous predictor intervals are varied from four to ten. An optimal first predictor is selected, which meets (in order) one of the following requirements:

a. the lowest CE value of all the potential predictors, or

b. the highest PP value of all potential predictors.

After selecting a first predictor for each of the equally populous intervals, the corresponding VISCAT I, II and III threat and AO scores are calculated for both dependent and independent data sets from the MAXPROB II strategy. Then the optimal equally populous predictor interval is selected such that it is the smallest interval to maximize the dependent data set's adjusted AO and independent data set's adjusted VISCAT I threat score (Appendix D).

Next, a functional dependence test of the first predictor against the remaining potential predictors is run. Subsequent predictors are selected only if:

a. the AO value increased over that at the preceding level, and

b. the selected predictor must have the lowest functional dependence and root-sum-square functional dependence of all the remaining potential predictors.

After completing the predictor selection stage, Monte Carlo significance testing is performed to see if the results are significant compared to random chance. Functional dependence/root-sum-square functional dependence, AO and A1 statistics are calculated for 100 randomly generated sets to determine the 5 and 96 percentile points of A1 and AO, denoted as 'A1(05)', 'AO(96)', respectively. The developmental model results are considered to be

significant if:

a. A0 is greater than or equal to A0(96), and

b. A1 is less than or equal to A1(05), and

c. the functional dependence value for a selected predictor is less than functional dependence 96 percentile level FD(96) (determined by the Monte Carlo procedure, above).

Model development continues until the fifth predictor level when computer storage limitations preclude further addition of predictors. Once complete, contingency tables of forecast versus observed visibility category are constructed for both dependent and independent data sets. Threat and skill scores are computed and compared.

E. THE PDM VS. PR METHODS

The PDM method and the PR methods can be shown to be equivalent in the discrete setting; it is in the non-discrete setting that they differ by virtue of fitting one or the other with analytic versions of discrete probabilities. The MAXPROB approaches make a prediction based on the probability distribution of the categories for a given predictor value, whereas the PDM method discriminates between the probabilities of the categories in a predictor space. In the PDM method, analytic functions are fitted to the category subsets of predictor space and comparisons are made between these probabilities at each given predictor value. Thus, more continuous information is available when the data are sparse in this method than with

the MAXPROB approach (although the latter, too, may be fitted with analytic probability models). Both of these methods should have an advantage over more traditional linear regression techniques whenever the data shows nonlinear rather than linear trends over the predictor space, since these methods would tend to follow the curve of the data, instead of trying to fit a straight line (or hyperplane) to them. The more predictor categories that are used and the more nonlinear the predictand/predictor relation, the greater is the anticipated advantage of PDM over linear regression.

V. RESULTS

The results of the Principal Discriminant Method (PDM) experiments, as outlined in Chapter IV and Appendix A, are presented herein. They are arranged by oceanic homogeneous area and model output period. Fig. 1 displays the individual oceanic homogeneous areas for FATJUNE 1983. Tables I through IV identify the number of observations in each visibility category by prediction interval (i.e., TAU) and homogeneous area.

The results are further clarified by the corresponding figures in Appendix G, which provide comparisons of PAO and dependent and independent AO scores versus the number of predictors chosen for that particular data set. The models for each set terminated due to established model constraints and not due to computer system storage restrictions. Note that dependent AO scores were not available at the first predictor level due to programming time and constraints. Future experiments could include this information. Thus, the dependent AO data start with the second predictor. The chosen predictors are listed in the order of selection. Contingency tables resulting after the selection of the final predictor are included for both dependent and independent sets. In general, independent AO (testing) scores are lower than the dependent (training) AO scores.

Even though the training and testing sets are representative of the same population, their points are scattered differently. This difference, in general, leads to a decrease in the AO scores from the dependent (training) set to the independent (testing) set. However, in a number of cases, the independent AO score is higher than the PAO score at the first predictor level. Likewise, the dependent AO score is higher than the PAO score at the second predictor level for some cases. Although, on average, one would expect the reverse to be true, the scatter of the individual test scores could occasionally lead to higher AO scores than PAO scores. The steady decline of AO scores for the first few predictors is also a common occurrence. While the PAO score continues its steady ascent (as required by the method to justify the addition of the next predictor) the AO scores shows more erratic behavior, exhibiting the instability of the method. However, when the criteria test was changed, as will be described later, the resulting AO values show a closer relationship to the PAO scores and hence greater stability. Stability is desired in a model or else its forecasts are of little value. To determine exactly why the method is stable or unstable, carefully controlled experiments would have to be performed with artificial data sets.

When comparing the results of the PDM model to the maximum probability and natural regression strategies of the

PR models, it was noted that the PR models provided higher scores in almost every case for all scoring techniques. This difference may be due to the composition of the data sets themselves, the separation of the data into training-testing pairs, some aspect of the methodology or a programming error. However, without conducting experiments on carefully constructed artificial data sets it would be impossible at this point to state a conclusive reason for the difference. One PDM experiment which was conducted at the end of the research did give comparable results to the PR methods and will be discussed in more detail later as will any other exceptions to the general finding stated above. Specific numerical values from the work of Karl (1984) and Diunizio (1984a), along with the corresponding PDM results, are presented in Table V.

A. NORTH ATLANTIC OCEAN, AREA 2

Area 2 encompasses a geographic region extending from the southeastern tip of Newfoundland, across the North Atlantic Ocean to the eastern coast of England, north/northeast to include most of Iceland, and back to the Canadian coast north of Newfoundland (Fig. 1).

1. Area 2, TAU-00

Results for this case are shown in Fig. 6. Five predictors were selected. The dependent AO score rises slightly between predictors two and three, and then roughly

parallels the independent A0 score. The independent A0 score does not show an increase over its initial value until the addition of the fifth predictor. The PDM model outperforms the PR model in the following scores (Table V):

a. TS2 scores for both dependent and independent sets are higher than for either MAXPROB I or MAXPROB II, thus showing better skill in forecasting VISCAT II.

b. The TS12 score is higher for the dependent set than either MAXPROB I or MAXPROB II.

2. Area 2, TAU-24

A variety of experiments were performed on this case. In addition to the standard application of the PDM techniques afforded the other cases, two additional three-category experiments and a two-category experiment were performed, as detailed in paragraphs a, b, and c below.

a. Set Composition Experiments

To determine the effect of the random composition of training/testing set pairs on the results, three distinct sets (2(A,B,C)) were created.

Sets 2(A,B,C) follow a similar pattern for the PA0 scores, except that sets 2(B) and 2(C) could not support more than five predictors, while the model for set 2(A) finally terminated with the seventh predictor (Fig. 7). The first five predictors were the same in all three cases. The dependent A0 scores (Fig. 8) follow a different pattern in each case (one (A) declining to predictor four and then increasing and decreasing once more, one (B) declining

steadily, and one (C) declining to predictor three and then increasing and decreasing once more) which is fairly well paralleled by the independent A0 scores (Fig. 9). Ideally, the curves in Figs. 8 and 9 should be as closely spaced as those in Fig. 7. Presumably, these scattered curves are showing giving information about the noise inherent in the observed visibility data sets. Also, they may indicate that PA0, PA1 must be redefined so that they may more realistically anticipate these scatterings of the A0, A1 scores. Separate figures for each set are found in Figs. 10, 11 and 12.

The PDM vs. PR results found for area 2, TAU-00 hold true at TAU-24 also.

b. Criteria Experiments

To determine the effect of altering the criteria for splitting data swarms in predictor space during the decomposition phase, two methods were tried. The first entailed changing the critical λ value from $\lambda(96)$ to $\lambda(98)$. The second eliminated Monte Carlo methods entirely and created a new value, λ', where λ' is the ratio of the largest eigenvalue (associated with the data swarm's covariance matrix) to the average of the remaining eigenvalues. For the λ' experiments, the set was split if $\lambda'>2$.

The criteria tests, which were all performed on set 2(A), show that changing the critical value from $\lambda(96)$

to $\lambda(98)$ leaves the PAO pattern basically unchanged. (Note that the same seven predictors were used in each of the criteria experiments.) The pattern for the λ' curve is much different, exhibiting a slower rise to the sixth predictor and then a large jump at the end, surpassing the results of the other criteria tests (Fig. 13). The major difference is in the behavior of the dependent and independent AO scores (Figs. 14 and 15). The $\lambda(96)$ test curve in Fig. 14 shows a sharp decline in the dependent AO score to the fourth predictor, an even sharper rise at the fifth predictor and decline thereafter. These scores are mirrored by the lower scoring independent AO's in Fig. 15. Both sets of scores are considerably less than the PAO scores of Fig. 13. The $\lambda(98)$ test gives a more stable version of the same pattern. Unlike the first two tests, the λ' test produces dependent AO scores in Fig. 14 quite similar to Fig. 13's PAO score through predictor six, with independent scores following a roughly similar pattern without a major loss in zero-error skill. These results show much greater stability than for any other experiments conducted and thus show the most promise for a continued investigation of the PDM method. The dependent and independent AO scores for the λ' version of PDM are comparable to those of the PR methods. Some of the skill scores are higher for PDM and some for PR. The point here is that "fine tuning" the criteria cut-off (from $\lambda'>2.0$ to some other value) could result in superior

scores overall. The $\lambda(98)$ and λ' cases are treated individually in Figs. 16 and 17. Once again, in comparing the curves in Figs. 16 and 17, we see that the λ' version of PDM produces much more stable and somewhat higher scores than the $\lambda(98)$ version.

c. Two-Category Experiments

The two-category cases (Chapter III.A.2) provide quite different final results when compared with each other, even though the general pattern was not much different between Case X and Case Y(A). (Note that there are three versions of Case Y, i.e., Y(A,B,C). All comparisons between Cases X and Y were done with the Y(A) data set.) The results for Case X are shown in Fig. 18. The model terminated at the fifth predictor level with the same five predictors as for the other Area 2, TAU-24 cases. Both dependent and independent AO scores decline through predictor number three, then slowly increase to a level much below their respective initial AO scores.

The three Case Y sets exhibit the same similarities in the PAO scores as the three-category cases (Fig. 19). Again, the AO scores (Figs. 20 and 21) tend to show a pattern of decline followed by increasing scores. However, in these two-category cases, the independent AO scores are very close to the dependent AO scores and they are considerably higher than for the the three-category

cases. Individual results for each case are presented in Figs. 22, 23 and 24.

Case X does not show AO scores appreciably higher than the AO scores from the three-category case. This might indicate that the data do not support the Case X VISCAT divisions any more than for the three-category case. However, Case Y does show significantly higher AO scores than the three-category case. This is more in line with the expected result; expected since it ought to be easier to forecast for two categories than for three under any circumstances. This result seems to indicate that the Case Y VISCAT divisions are supported by the available data, i.e., that it may be more feasible for on-board observers to discern between less than or greater than 2 km visibility, than less than or greater than 4 km visibility.

3. Area 2, TAU-48

Results for this case are shown in Fig. 25. Four predictors were selected. The dependent AO scores stay virtually constant for all predictors. The independent AO scores show a continuous decline with each additional predictor. The PDM shows higher dependent threat scores and an independent TS2 score when compared to MAXPROB I.

B. NORTH ATLANTIC OCEAN, AREA 3W

Area 3W borders the United States' eastern seaboard from the vicinity of Cape Charles, Virginia to the southeastern

tip of Newfoundland. The area encompasses a large portion of the Georges Banks region and extends to approximately 45° W longitude (Fig. 1).

1. <u>Area 3W, TAU-00</u>

Results for this case are shown in Fig. 26. Five predictors were chosen. Once again, both dependent and independent AO scores decline until the addition of the fifth predictor, at which point they surpass their initial values.

2. <u>Area 3W, TAU-24</u>

The results for this case are shown in Fig. 27. Three predictors were selected. In this case, the independent AO score increase with the addition of each predictor, while the dependent AO score decreases. This pattern is not seen in any other case.

3. <u>Area 3W, TAU-48</u>

The results for this case are shown in Fig. 28. Seven predictors were chosen. The dependent and independent AO scores decline until the addition of the fifth predictor where they reach their maximums. The sixth predictor shows another decline and the seventh an increase. The independent TS2 score in the PDM model equals that of the PR model.

C. NORTH ATLANTIC OCEAN, AREA 4

Area 4 encompasses a broad region of the North Atlantic Ocean which is generally to the south of area 2 and east and southeast of area 3W. This area's southern border reaches to the northeastern tip of Portugal and extends northward through the English Channel to encompass the southern portion of the North Sea (Fig. 1).

1. Area 4, TAU-00

The results for this case are shown in Fig. 29. Only two predictors were chosen for this model. The independent AO score declines after the addition of the second predictor. The dependent AO score shows no trend since only one value was available.

2. Area 4, TAU-24

The results for this case are shown in Fig. 30. Four predictors were chosen. The dependent and independent AO scores declined until the addition of the fourth predictor. At that point, they are larger than at their initial predictor stage. The dependent and independent results are almost identical which is a rare result. The PDM model shows higher scores for all dependent threat scores compared to MAXPROB I and the independent TS2 score from MAXPROB I.

3. Area 4, TAU-48

The results for this case are shown in Fig. 31. Two predictors were chosen. The independent AO score increases

from the first to the second predictor. No trend is available for the dependent AO score.

VI. CONCLUSIONS AND RECOMMENDATIONS

A. CONCLUSIONS

The primary objective of this study is to evaluate the Principal Discriminant Method (PDM) [Preisendorfer, 1984], to compare those results to the maximum probability and natural regression schemes [Preisendorfer, 1983a,b,c] examined by Karl (1984) and Diunizio (1984a), and to propose a viable statistical forecasting scheme suitable for eventual employment in an operational U. S. Navy marine visibility MOS forecasting system. In general, the PDM model, using the $\lambda(96)$ criteria for decomposing sets, was outperformed in all measures of effectiveness by all of the PR schemes.

However, the version of the PDM model which used the λ' criterion for splitting predictor category sets during decomposition showed very promising results (cf., 2b in V.A. and Table V). The A0/A1 scores for both dependent and independent sets were very close to those of the PR models. Perhaps, this is because the λ' criterion is a better judge of the geometry of the data sets than the Monte Carlo $\lambda(96)$ criterion. The result is that the information contained in the data set is more readily available in the λ' method than for the other predictor space category splitting methods.

B. RECOMMENDATIONS

The following recommendations are offered to future researchers:

1. The decision criteria for splitting data swarms in the decomposition phase need further examination. Indeed, it is the novel use of principal component analysis for this purpose that distinguishes the present discriminant method from other such methods in the literature. The λ' criterion appears to be a step in the right direction (note 2b in V.A.). Further research should center on determining the best value against which to test the λ value, or still other ways of splitting the overly-elongated category subsets of predictor space.

2. Create carefully controlled artificial data sets on which to apply all of the Preisendorfer models (MAXPROB, natural regression, PDM) to determine where and why they break down or excel. Also, using the same artificial data, simultaneously test regression, especially linear, along with the various threshold models.

3. Remove from further consideration the $\lambda(96)$ and $\lambda(98)$ critical score criteria in the decomposition phase of the model.

4. Test the PDM model, using the entire FATJUNE 1983 data set as the training set and the entire FATJUNE 1984 data set as the testing set, or vice versa.

5. Use winter data for a set of experiments to determine if the results are similar to that of the summer season.

6. Use a night-time data set (0000 GMT) in the North Atlantic area to test the expected deterioration of all schemes relative to daytime conditions.

APPENDIX A

A DISCUSSION OF THE STATISTICAL PROCEDURES PROPOSED BY PREISENDORFER (1984) FOR THE FORECASTING OF ATMOSPHERIC MARINE HORIZONTAL VISIBILITY USING MODEL OUTPUT STATISTICS

I. INTRODUCTION

The following discussion is based upon an unpublished note by Preisendorfer (1984). The note develops the Principal Discriminant Method (PDM) of forecasting and suggests how to link the output of numerical weather prediction model output parameters with observed fields to produce model output statistics (MOS) prediction schemes. The application of his methodology to MOS forecasting is as follows:

1. Generate suitably lagged predictand/predictor pairs of data. The predictors are drawn from the United States Navy Fleet Numerical Oceanography Center's Navy Operational Global Atmospheric Prediction System (NOGAPS) model output. The predictands are drawn from synoptic ship visibility observations provided by the Naval Oceanography Command Detachment, Asheville, North Carolina.

2. Separate the predictand data into visibility categories. Construct predictand/predictor pairs based on the predictand visibility category values. Partition the space of predictor values into category subsets.

3. Fit a probability density function to the category subsets of predictor space. This task is facilitated by using a succession of principal component analyses of the category sets in predictor space.

4. Based on the probability density functions for the training set, find the potential class errors, PA0, PA1.

5. Based on the probability density functions and utilizing testing set data, find the actual class errors, A0, A1.

6. Pick as the first predictor the one with the smallest averaged P-value (a measure of separation between two probability density functions) and largest PA0 value.

7. Correlate a potential predictor with the set of already selected predictors, selecting as the next predictor the one which is least correlated with the already-selected set.

8. Repeat steps 1-5 and 7 until all predictors are chosen.

II. SINGLE PREDICTOR STAGE

A. THE PREDICTOR/PREDICTAND PAIR*

For each individual data point I (I=1,NTRN, the number of points in the training set) there is a predictand value NTRPY(I) and its corresponding predictor values TRNPX(I,KX) where KX=1,KP, the total number of predictors under consideration. For this study, the NTRPY(I)'s represent visibility while the TRNPX(I,KX) may be, e.g., the vapor pressure at 925 mb, or surface moisture flux, etc.

B. THE DISCRIMINANT SET

The discriminant diagram, Fig. 2a, for the data, shows histograms indicating to which predictand category a given

---

*The notation herein follows that of the corresponding computer code.

predictor value is assigned. Thus the triangles are for category 1, circles for category 2, squares for category 3. In Fig. 2b, these histograms are separated vertically to form the discriminant set. As the points in the data set are considered (i.e., as I changes), the TRNPX(I,KX) value moves irregularly about on the horizontal axis while the corresponding NTRPY(I) moves similarly among the three levels of the vertical axis now occupying category 1, then category 3, and so on. A point pair is shown in an instantaneous position in Fig. 2b. There are NTRN such pairs in the dependent (training) discriminant set and NTST such pairs in the independent (testing) discriminant set. The diagram in Fig. 2b stands for either of these two discriminant sets.

C. CATEGORY SUBSETS OF PREDICTOR SPACE

Looking at the discriminant set (Fig. 2b), notice the subset of predictor points associated with category one. This is XCAT1(I1,KX), the rightmost pairs of points on the first level (which is simply a copy of the horizontal axis). Similarly, XCAT2(I2,KX) contains the middle pairs and XCAT3(I3,KX) the leftmost pairs. Each predictor point of the training set is assigned to a predictand in a particular category. Thus predictors corresponding to the training predictand values in categories 1,2 or 3 are assigned to XCAT1, XCAT2 or XCAT3 respectively. I1, I2 and I3 represent

the index of values in the respective categories. KX identifies the predictor (e.g., vapor pressure at 925 mb., etc.).

D. FITTING THE PROBABILITY DENSITY FUNCTION

For this study, the Gaussian probability density function (PDF) was chosen to be fitted to the category subsets of the predictor space. However, one might consider using other PDF's if they were more suitable for a given data set.

The one dimensional Gaussian PDF for category J is:

$$\text{PHIJ}=(2\pi)^{-\frac{1}{2}}*(\text{SIGJ})^{-1}*\text{EXP}(-0.5((\text{X}-\text{AVGJ})**2/\text{VARJ})$$

where J=1,2,3, and

AVGJ=average

SIGJ=standard deviation

VARJ=variance

of the set of points defined by XCATJ(IJ,KX), IJ=1,NXJ for each predictor indexed by KX. The fitted curves may appear as in Fig. 2c.

E. CLASS ERRORS

An indication of how well a prediction method is doing is to count the number of predictions that are correct (zero-class errors) and the number of predictions that are off by one category (one-class errors). This is done two ways. The potential zero-and one-class errors, PA0 and PA1, are determined using the probability functions fitted to the

category subsets of the training set. The actual zero-and one-class errors, A0 and A1, are determined using the testing set.

1. Finding the probabilities

Form the array

ANU(M,J)=PHIJ(TRNPX(M,KX)), KX fixed,

where J=1,2,3

TRNPX is the training set function which assigns to (M,KX), a predictor value

M=1,...,NTRN the indexes of points in the training set

KX=1,...,KP the set of predictors' indexes

Let

$$SNU(M)=\sum_{J=1}^{3} ANU(M,J)$$

and define the probabilities:

PRB(M,J)=ANU(M,J)/SNU(M).

2. Finding PA0,PA1

Find the maximum of the set of probabilities PRB(M,J),J=1,3. Let this be PRB(M,J(M)) for each M=1,NTRN.For example, if of PRB(M,1), PRB(M,2) and PRB(M,3), the maximum value occurs for PRB(M,2), then J(M)=2. In practice, this would result in predicting category 2. Then define

$$PA0=\frac{1}{NTRN}\sum_{M=1}^{NTRN} PRB(M,J(M))$$

$$PA1=\frac{1}{NTRN}\sum_{M=1}^{NTRN}[APRB(M,J(M)) + APRB(M,J(M)+2)]$$

$$PA2= 1 - (PA0 + PA1)$$

where APRB(M,1)=0

APRB(M,2)=PRB(M,1)

APRB(M,3)=PRB(M,2)

APRB(M,4)=PRB(M,3)

APRB(M,5)=0

The APRB arrays allow for easier calculation of PA1 since array indexing does not allow for PRB(M,0) terms, for example.

The higher the PA0 values and the lower the PA1 values, the potentially better the predictor PX(I,KX) may predict PY(I). Therefore, a potentially good predictand-predictor pair has large PA0 and small PA1 values.

3. Finding A0,A1

A0 and A1 are the actual zero- and one-class errors produced by the model when the predictor values of the testing set are given to the previously established probability density functions, i.e., the PHIJ's. Using the same strategy as for PA0,PA1 make a prediction for the predictand value and then compare it with the actual predictand value from the testing set. With each correct prediction or one-class error, the totals of A0 or A1 increase by one unit, respectively:

A0=(1/NTST)(TOTAL ZERO-CLASS ERRORS)

A1=(1/NTST)(TOTAL ONE-CLASS ERRORS)

F. SCREENING AND RANKING CATEGORY SUBSETS

1. Separability of Category Subsets

Unless the category subsets are well separated from each other, the predictions will not have much skill.* As a measure of separability, the P-statistic of each distinct pair of categories is found for each predictor using BMDP Statistical Software program P7D [University of California, 1983]. For the three-category case at hand, this provides three P-values which are then averaged to provide a single mean P-value for each predictor. These are then ranked smallest to largest: the smaller the value the better separated are the data heaps in the category subsets. The first chosen predictor is thus the one with the smallest mean P-value. (Other measures of separability exist. See, e.g., the potential predictability (PP) measure in Preisendorfer (1983a).

2. PAO scores

In the event that more than one predictor has the smallest mean P-value, then the first predictor is chosen by selecting from among those predictors the one with the largest PAO score.

---

*Unless category set separation is present, it is unlikely that any method of prediction of the given predictand from the given predictors will be skillful. It is this feature of the prediction problem that discriminant methods, such as the present one, isolate most clearly: if category probability density curves are well separated and the training set is representative of the data set, then high forecast skill is assured.

III. MULTIPLE PREDICTOR STAGE

A. CORRELATIONAL SCREENING OF PREDICTORS

Suppose we have K-1 predictors selected, where K=2,..,KP and KP is the total number of predictors. Let the selected predictors be TRNPX(I,KX), KX=1,..,K-1. So, if there is one chosen predictor we have TRNPX(I,1), I=1,NTRN. Let the remaining set of predictors be denoted TRNPW(I,KW), KW=1,...,L where L=KP + 1 - K. Let CORR[KW,KX] denote the correlation between the KXth chosen predictor and the KWth unchosen predictor. Since the correlation is a measure of the distance between a chosen and an unchosen predictor, we are looking for the smallest value of the correlation since a smaller value indicates that the unchosen predictor is farther from (i.e., less dependent on) a chosen predictor.

Therefore, let

$$C(KW)=\max_{KX=1,K-1}\{\text{ABS CORR }[KW,KX]\}$$

This gives (an inverse) measure of the distance of the KWth potential predictor from the set of chosen predictors. The smaller C(KW) is, the larger the distance. The next predictor chosen for consideration is the one with the smallest C(KW) value.

B. THE K-DIMENSIONAL DISCRIMINANT SET

Once the Kth predictor is added, there are two sets, one training and one testing, of K predictors in the form of a vector

$\underline{VECPX}(I)=(PX(I,1),\ldots,PX(I,K))$

in the Euclidean K-space E_K. As index I changes, $\underline{VECPX}(I)$ moves about in E_K, as does the predictand array NTRPY(I). The set of all ordered pairs ($\underline{VECPX}$(I),NTRPY(I)), I=1,NTRN is the present discriminant training set and is a general (k-stage) version of section II.B. above. ($\underline{VECTS}$(I),NTSPY(I)),I=1,NTST is the discriminant testing set.

C. CATEGORY SUBSETS OF PREDICTOR SPACE

As in II.C. above, category subsets of the K-dimensional predictor training vector are formed, based on the value of the associated predictand value. The net result is three subsets of E_K defined by the three swarms of points

$\{\underline{XCATJ}(I): \quad I=1,NXJ\}$

where J=1,2,3, and NXJ is the number of points in the subset. Here $\underline{XCATJ}(I)=[XCATJ(1,I),\ldots,XCATJ(K,I)]^T$. On these three subsets of E_K we fit the K-dimensional Gaussian PDF's. However, these data swarms are not usually distributed normally which brings about the next step.

D. BINARY PRINCIPAL DECOMPOSITION OF THE CATEGORY SUBSETS

Let $X_J = \{XCATJ(I): I=1,\ldots,NXJ\}$, J=1,2,3, be the Jth category subset of E_K. A general picture of X_J for the case K=2 is in Fig. 3. The shape of X_J may possibly be elongated and curvilinear. Since the most variance of the subset is along the unit vector $\underline{e}_1$ at 0, this suggests that we form a principal component decomposition of the swarm X_J of NXJ points in E_K where J=1,2,3. The principal component decomposition is well-suited to find this direction $\underline{e}_1$ of greatest variance. This is done in the following steps.

1. Recall that in III.C., the data sets forming the predictors were standardized. Next, go on to find the centroid <u>AMEANJ</u> of each <u>XCATJ</u> in E_K. This is the centroid point shown as 0 in Fig. 3. By definition,

$$\underline{AMEANJ} = \frac{1}{NXJ} \sum_{I=1}^{NXJ} XCATJ(I)$$

The Lth component of AMEANJ is

$$AMEANJ(L) = \frac{1}{NXJ} \sum_{I=1}^{NXJ} XCATJ(I,L)$$

where L=1,...,K.

2. Form the covariance matrix <u>SJ</u> of the X_J data swarm. Thus, first center the points <u>XCATJ</u>(I) on the mean <u>AMEANJ</u> of X_J:

$$XJ(I) \equiv XCATJ(I) - AMEANJ, \quad I=1,\ldots,NXJ$$

i.e., in component form

$$XJ(I,L) = XCATJ(I,L) - AMEANJ(L)$$

$$I=1,\ldots,NXJ; \; L=1,\ldots,K$$

Then the entry SJ(L,M) of <u>SJ</u> in its Lth row and Mth column

is:

$$SJ(L,M)=\frac{1}{NXJ-1}\sum_{I=1}^{NXJ}XJ(I,L)XJ(I,M)$$

for L,M=1,...,K and for categories J=1,2,3.

3. Find the eigenvalues and eigenvectors of the covariance matrix SJ(L,M). Sort the eigenvalues from high to low, and arrange their corresponding eigenvectors similarly.

4. Compute A(I), the principal components from

$$A(J)=\sum_{L=1}^{NXJ}XJ(I,L)e_1(L)$$

where $\underline{e}_1=[e_1(1),\ldots,e_1(NXJ)]^T$ is the eigenvector corresponding to the largest eigenvalue of the data swarm currently under consideration.

The following steps describe how the above information is used in decomposing the data swarms to a terminal state for use in the multi-predictor PDF's. See Fig. 3 for level 0 of the splitting procedure.

5. Decision to split subsets at level 1:

a. For K predictors and a set $X_J(a_1,\ldots,a_\ell)$ of n_J points:

1) If $n_J \leq K+1$, where K=number chosen predictors, set $T_J(a_1,\ldots,a_\ell) = X_J(a_1,\ldots,a_\ell)$. This set is terminal because any further splits of the set will lead to degeneracy. In fact, if $n_J<K$, set PHIJ=0 for this set since in this case only trivial covariance matrices will be found.

2) If $n_J > K+1$, go to b.

b. Perform principal component analysis (PCA) of the point swarm $X_J(a_1,\ldots,a_\ell)$ in E_K. Determine the eigenvalues

$\ell_1, \ldots, \ell_k$, where ℓ_1 is the largest and ℓ_k is the smallest. Let $\ell = \sum_{i=1}^{k} \ell_i$. Compute $\lambda = \ell_1/(\ell - \ell_1)$. Go to c.

c. Perform a Monte Carlo experiment to determine if λ is significantly large. That is, randomly generate a duplicate of the data swarm under consideration, normalize the data and find the centroid, covariance matrix and eigenvalues. Let $\ell_1^{(i)} \geq \ell_2^{(i)} \geq \ldots \geq \ell_k^{(i)}$ be the ordered set of eigenvalues resulting from the ith Monte Carlo experiment, $i=1,\ldots,100$. Let $\ell_{.}^{(i)} = \sum_{j=1}^{k} \ell_j^{(i)}$ and set $\lambda(i) \equiv \ell_1^{(i)}/(\ell^{(i)} - \ell_1^{(i)})$. Arrange the $\lambda(i)$ in ascending order, so that, after relabeling, $\lambda(1) \leq \lambda(2) \leq \ldots \leq \lambda(96) \leq \ldots \lambda(100)$.

1) If $\ell_k = 0$, for any J=1,2,3 set PHIJ=0.

2) If $\lambda < \lambda(96)$, set $T_J(a_1, \ldots, a_\ell) = X_J(a_1, \ldots, a_\ell)$. This is the terminal case. Go to the next swarm awaiting decomposition.

3) If $\lambda(96) \leq \lambda$, go to d.

d. A split is performed by setting

$$X_J(a_1, \ldots, a_{\ell 0}) = \{\underline{X}(I): \underline{X}(I) \in X_J(a_1, \ldots, a_\ell) \text{ and } A_1(I) \leq 0\}$$

$$X_J(a_1, \ldots, a_{\ell 1}) = \{\underline{X}(I): \underline{X}(I) \in X_J(a_1, \ldots, a_\ell) \text{ and } A_1(I) > 0\}$$

where $\underline{X}(I)$ is a point (k-tuple) of numbers in E_K. When splits are completed on all levels, we have a set of terminal nodes $T_J(a_1, \ldots, a_\ell)$. See Fig. 4.

E. FITTING PROBABILITY DENSITY FUNCTIONS TO EACH TERMINAL NODE

Denote the terminal nodes by '$T_J(I)$' which is the name of the Ith terminal node found by successive splits of X_J in

E_K. (Note: if the terminal node results from a degeneracy or from the case $\ell_k=0$, then no further work is done since PHIJ=0 in those cases for all points.) Establishing the following notation:

AVGJ(I)=centroid of the terminal swarm of points $T_J(I)$

$\underline{C}_J(I)$=KxK covariance matrix of $T_J(I)$

$DET_J(I)$=determinant of $\underline{C}_J(I)$ where

$DET_J(I)=\prod_{r=1}^{k}\ell_r$, ℓ_r= eigenvalues of $\underline{C}_J(I)$.

Then the required probability density function is

$$PHIJ(I,\underline{X})\equiv[2\pi]^{-k/2}*[DET_J(I)]^{-\frac{1}{2}}*EXP[-0.5*(X-AVGJ(I))^T\underline{C}_J^{-1}(I)(\underline{X}-AVGJ(I))]$$

where I runs over all terminal nodes associated with category subset X_J

$\underline{X}$ is an arbitrary point in E_K

$\underline{X}$ - $\underline{AVGJ}$(I) is a k-component column vector in E_K, 'T' denoting transpose

$\underline{C}_J^{-1}(I)$ is the inverse of the covariance matrix $\underline{C}_J(I)$.

This results in a set of three probability distributions PHIJ(I,$\underline{X}$), J=1,2,3 and forms the present model over each X_J, after suitably assembling these PHIJ(I,$\underline{X}$) values.

F. ASSEMBLING THE PHIJ(I,$\underline{X}$) ON EACH X_J

Let $n_J(I)$ be the number of points in $T_J(I)$. Then

$\sum_{I=1}^{M_J} n_J(I)$=NXJ, the number of points in X_J

where M is the number of terminal nodes arising in X_J.

Define

$a_J(I)=n_J(I)$/NXJ.

Then $\sum_{I=1}^{M_J} \alpha_J(I)=1$. Set $PHIJ(\underline{X})= \sum_{I=1}^{M_J} \alpha_J(I)PHIJ(I,\underline{X})$ for J=1,2,3, $\underline{X}$ in E_K. This is the desired model.

G. CLASS ERRORS

These are made from the new versions of PRB(M,J(M)) computed as in section II.E. above.

H. FINAL SCREENING TESTS FOR CANDIDATE PREDICTOR PX(I,K)

1. Using BMDP program P3D compute the P-value for each of the three possible pairs of PDF's for the three categories. Average these values and find $\bar{P}$.

2. Compare the new PA0 and PA1 values with those found for the previous run with one less predictor.

3. Compare the new PA0 to the null hypothesis.

Accept PX(I,K), the Kth candidate predictor, if each of the following hold:

*a. $\bar{P} \leq .05$

b. $PA0(K-1)<PA0(K)$, $PA1(K) \leq PA1(K-1)$

c. $PA0>PA0(null)$

Here PA0(null) is the upper limit of the 95% confidence interval, as found in Appendix B.

If these conditions are not fully met, return to section III.A. and select the next potential predictor PW(I,KW) in line, until all potential predictors have been considered.

---

*In the original version of PDM [Preisendorfer, 1984], this step uses the potential predictability (PP) criterion.

Once the model is finished, that is all potential predictors have been considered, then compute the actual A0(I) and A1(I) scores using the testing set.

IV. EXAMPLE

An example is helpful in understanding how the method works in practice. The results presented here were obtained by applying the method to a set of 200 points taken from the Area 2, TAU-24 data set. The example will extend through one level of the multi-predictor stage, i.e., through the selection and acceptance of a second potential predictor.

A. SELECTION OF FIRST PREDICTOR

The first step towards identifying the first predictor is to run the BMDP Statistical Software program P7D [University of California, 1983], to find the average P-value for each predictor. In this case, there were several predictors for which the average P-value was 0.0. Therefore, (see note 2 of II.F.) the results showing the PA0, PA1, A0 and A1 scores for each predictor (if used as the first predictor) had to be consulted before the choice was made. The chosen predictor was E850 because of all the predictors with an average P-value of 0.0, it had the largest PA0 score (.51).

Predictor E850 was then correlated with the remaining potential predictors. The potential second predictor chosen was DEDP because it had the smallest correlation coefficient when correlated with E850.

B. THE SECOND PREDICTOR STAGE

With the first predictor chosen and a candidate second predictor ready for consideration, it was necessary to begin the principal component analysis (PCA) of the data swarm in anticipation of creating the probability density functions.

When broken into the three categories corresponding to the visibility groupings, the categorized data sets contained the following numbers of points:

XCAT1--14

XCAT2--14

XCAT3--172

The decomposition of the first category subset (XCAT1) will be explained in detail, since it is small. Fig. 5 presents a pictorial representation of the following steps in the K=2 (predictor) stage:

1. Consider XCAT1 first. For this swarm, $\lambda > \lambda(96)$. Therefore, the swarm must be split using PCA. The two new sets are $X_1(0)$ with 6 points and $X_1(1)$ with 8 points.

2. Consider the swarm $X_1(0)$. Since $\lambda < \lambda(96)$ in this case, the set is terminal, i.e., $T_1 = X_1(0)$. No further decomposition is performed on this set.

3. Consider the swarm $X_1(1)$. Here, $\lambda>\lambda(96)$, so the swarm is further decomposed into $X_1(10)$ with 5 points and $X_1(11)$ with 3 points.

4. Next $X_1(10)$ is considered. Since $\lambda>\lambda(96)$, this swarm is further decomposed into $X_1(100)$ with 4 points and $X_1(101)$ with 1 point.

5. Next $X_1(11)$ is considered. Since this swarm has only 3 values, and 3 K+1, this swarm is terminal. Thus, $T_2=X_1(11)$.

6. The data swarm $X_1(100)$ with 4 points is found to have $\lambda>\lambda(96)$ and therefore, it is terminal. Set $T_3=X_1(100)$.

7. The set $X_1(101)$ has only 1 point. Since 1 K, this set is degenerate. Although $T_4=X_1(101)$, for this terminal set PHIJ=0 for all values of X. Therefore, it is not considered when building the probability density functions.

Thus for XCAT1, there are three useable terminal sets. Similarly, there are two for XCAT2 and fourteen for XCAT3.

Once the PHIJ's are formed and probabilities computed, potential class errors are computed and compared to the potential errors found at the one predictor level. The new PA0 (.67) is greater than at the one-predictor level (.51) and the new PA1 (.27) is lower than at the one predictor level (.39). With part of the selection criteria satisfied, the average P-value using both predictors was found using BMDP Statistical Software program P3D [University of California, 1983]. Since the average P-value (0) met the

significance criteria of being less than .05, a second requirement towards acceptance of the second predictor was met. Since PAO (.67) was greater than PAO(null)=.40, the third criteria was met and the second predictor DEDP was accepted.

APPENDIX B

NULL HYPOTHESIS SIGNIFICANCE TESTING

Following the work of Diunizio (1984a), Mr. Paul Lowe of NEPRF proposed that statistics such as AO and threat scores could be assigned normal probability distributions and, therefore, be subject to Null Hypothesis significance testing criteria. The assignment of the normal probability distributions is based upon the Central Limit Theorem. Diunizio (1984b) explored this technique and presented the subsequent results. This appendix presents the equations used in this study for significance testing.

When using three visibility categories, the null hypothesis is that the percentage correct will be .333 if only chance is involved. Using a 95% confidence test, we want to create an interval around the null hypothesis value such that values outside are considered to be significant.

Let P_0=.333

n=number of values in data set

$z_{\alpha/2}$ = 1.96 for 95% confidence interval

$(1 - \alpha = .95, \therefore \alpha/2 = .025)$

then $AA = P_0 - z_{\alpha/2}[P_0(1 - P_0)/n]$

$BB = P_0 + z_{\alpha/2}[P_0(1 - P_0)/n]$

where AA is the lower limit and BB is the upper limit of the confidence interval.

APPENDIX C

WORLD METEOROLOGICAL ORGANIZATION HORIZONTAL SURFACE VISIBILITY CODES

CODE	VISIBILITY(KM)
90	<0.05
91	0.05
92	0.2
93	0.5
94	1.0
95	2.0
96	4.0
97	10.0
98	20.0
99	50.0 or more

Note: The values given are discrete values (i.e., not ranges). If the observed visibility is between two reportable distances as given in the table, the code figure of the lower reportable distance shall reported.

APPENDIX D

<u>SKILL AND THREAT SCORES, DEFINITIONS</u> (Karl, 1984)

FORECAST			
3	R	S	T
2	U	V	W
1	X	Y	Z
	1	2	3

OBSERVED

Total = R + S + T + U + V + W + .X + Y   Z

P1 = (R+U+X)/Total   P3 = (T+W+Z)/Total

P2 = (S+V+Y)/Total   PN = greatest of P1, P2 or P3

Raw Scores

A0 = fraction correct = zero-class error = (X+V+T)/total

A1 = one-class error = (U+S+Y+W)/Total

A2 = two-class error = (R+Z)/Total

A0 + A1 + A2 = 1

TS1 = Threat score for visibility category I

= X/(R+U+X+Y+Z)

TS2   Threat score for visibility category II

= V/(S+V+Y+U+W)

TS12 = Threat score for visibility categories I and II

$= (X+V)/(Total-T)$

TS12 is designed to represent the skill of forecasting visibility categories I and II as separate categories, rather than their skill as a combined category, which would be (U+V+X+Y)/Total-T).

Adjusted scores

$AAO = (AO-PN)/(1-PN)$

$ATS1 = (TS1-P1)/(1-P1)$

$ATS2 = (TS2-P2)/(1-P2)$

$ATS12 = (TS12-(P1+P2))/(1-(P1+P2))$

APPENDIX E

NOGAPS PREDICTOR PARAMETERS AVAILABLE FOR NORTH ATLANTIC OCEAN EXPERIMENTS

I. Area: North Atlantic Ocean and Mediterranean Sea

Model output time: 1200GMT (TAU-00, TAU-24, TAU-48)
15 May--7 July 1983

Legend:

* * Parameters which were not used because they were considered physically unrelated to marine visibility.
* ** Parameters which were not used due to loss of significant digits during transfer from tape to mass storage.
* *** Parameters existing for TAU-24 and TAU-48 only.

A.

Model output parameter	Descriptive name of parameter
D1000	1000 mb geopotential height
D925	925 mb geopotential height
D850	850 mb geopotential height
D700	700 mb geopotential height
D500	500 mb geopotential height
D400 *	400 mb geopotential height
D300 *	300 mb geopotential height
D250 *	250 mb geopotential height
TAIR	Surface air temperature
T1000	1000 mb temperature

T925	925 mb temperature
T700	700 mb temperature
T500	500 mb temperature
T400 *	400 mb temperature
T300 *	300 mb temperature
T250 *	250 mb temperature
EAIR	Surface vapor pressure
E1000	1000 mb vapor pressure
E925	925 mb vapor pressure
E850	850 mb vapor pressure
E700	700 mb vapor pressure
E500	500 mb vapor pressure
UBLW	Boundary layer zonal wind component
U1000	1000 mb zonal wind component
U925	925 mb zonal wind component
U850	850 mb zonal wind component
U700	700 mb zonal wind component
U500	500 mb zonal wind component
U400 *	400 mb zonal wind component
U300 *	300 mb zonal wind component
U250 *	250 mb zonal wind component
VBLW	Boundary layer meridional wind component
V1000	1000 mb meridional wind component
V925	925 mb meridional wind component

V850	850 mb meridional wind component
V700	700 mb meridional wind component
V500	500 mb meridional wind component
V400 *	400 mb meridional wind component
V300 *	300 mb meridional wind component
V250 *	250 mb meridional wind component
VOR925 **	925 mb vorticity
VOR500 **	500 mb vorticity
PS	Surface pressure
SMF	Surface moisture flux
PBLD	Planetary boundary-layer depth
STRTFQ	Percent stratus frequency
STRTTH	Stratus thickness
SHF	Surface heat flux
ENTRN	Entrainment at top of marine boundary-layer
DRAG **	Drag coefficient (C_D)
PRECIP ***	Total amount (mm) of model precipitation in the last six hours
SHWRS ***	Total amount (mm) of model precipitation associated with cumulus convection in the last six hours
INSTAB ***	Boundary layer inversion instability
DIV925 ***	925 mb divergence

B. Derived Parameters

DTDP	Vertical gradient of temperature (1000-925 mb)
DEDP	Vertical gradient of vapor pressure (1000-850 mb)
DUDP	Vertical gradient of zonal wind (1000-850 mb)
DVDP	Vertical gradient of meridional wind (1000-850 mb)
RH	Surface relative humidity
TV	Virtual temperature
DDVDP	Vertical gradient of geopotential height (1000-850 mb)
DVRTDP **	Vertical gradient of vorticity (500-925 mb)
DUUPDP	Vertical gradient of zonal wind (300-500 mb)
DVUPDP	Vertical gradient of meridional wind (300-500 mb)
ESUM	Sum of vapor pressures (1000 & 850 mb)
EPRD	Product of vapor pressures (1000 & 850 mb)
EDIF	Difference of vapor pressures (1000-850 mb)

APPENDIX F

TABLES

TABLE I. A summary of 1200 GMT observations, 15 May--7 July 1983, North Atlantic Ocean homogeneous areas 2, 3W, 4: TAU-00

Area	DEP	IND	Total	Dependent VISCAT I	Dependent VISCAT II	Dependent VISCAT III	Independent VISCAT I	Independent VISCAT II	Independent VISCAT III
2	1915	952	2867	193	219	1503	67	87	798
3W	1532	756	2288	290	189	1053	118	102	536
4	3174	1597	4471	82	394	2698	26	197	1374

TABLE II. A summary of 1200 GMT observations, 15 May--7 July 1983, North Atlantic Ocean homogeneous areas 2(A,B,C), 3W, 4: TAU-24

Area	DEP	IND	Total	Dependent VISCAT I	Dependent VISCAT II	Dependent VISCAT III	Independent VISCAT I	Independent VISCAT II	Independent VISCAT III
2(A)	1721	842	2563	161	198	1362	46	86	710
2(B)	1686	877	2563	156	196	1334	44	85	748
2(C)	1723	840	2563	171	198	1354	54	76	710
3W	1384	683	2067	269	172	943	86	88	509
4	2852	1425	4277	74	364	2414	28	171	1226

TABLE III. A summary of 1200 GMT observations, 15 May--7 July 1983, North Atlantic Ocean homogeneous areas 2, 3W, 4: TAU-48.

				Dependent VISCAT			Independent VISCAT		
Area	DEP	IND	Total	I	II	III	I	II	III
2	1858	919	2777	179	226	1453	42	87	790
3W	1491	739	2230	280	191	1020	109	98	532
4	3047	1536	4583	99	410	2538	25	183	1328

TABLE IV. A summary of 1200 GMT observations, 15 May--7 July 1983, North Atlantic Ocean homogeneous area 2 (Case X, Case Y(A,B,C)): TAU-24.

Area	DEP	IND	Total	Dependent VISCAT I	Dependent VISCAT II	Independent VISCAT I	Independent VISCAT II
2X	1721	842	2563	214	1507	70	772
2YA	1721	842	2563	161	1560	46	796
2YB	1686	877	2563	156	1530	44	833
2YC	1682	881	2563	155	1527	43	838

TABLE V. A summary of skill scores obtained for dependent and independent data sets using the PR [Karl, 1984; Diunizio (1984)] and PDM methods on FATJUNE 1983 data from North Atlantic Ocean homogeneous areas 2, 3W and 4: TAU-00, TAU-24, TAU-48.

		DEPENDENT					INDEPENDENT				
Area/TAU	Method	A0	A1	TS1	TS2	TS12	A0	A1	TS1	TS2	TS12
2/00	MAXPROBI	.79	.11	.29	0.0	.19	.80	.11	.30	0.0	.20
	MAXPROBII	.79	.11	.29	0.0	.19	.80	.11	.30	0.0	.20
	NATREG	.97	.03	.92	.75	.86	.74	.20	.21	.09	.15
	PDM	.66	.29	.21	.24	.24	.59	.28	.05	.08	.06
3W/00	MAXPROBI	.99	.01	.95	.91	.95	.70	.16	.34	.15	.27
	MAXPROBII	.98	.01	.95	.92	.95	.66	.19	.33	.14	.27
	NATREG	.98	.02	.95	.84	.93	.65	.25	.32	.13	.24
	PDM	.67	.20	.28	.19	.27	.55	.25	.11	.07	.09
4/00	MAXPROBI	.97	.02	.72	.91	.81	.82	.15	.07	.15	.14
	MAXPROBII	.97	.02	.77	.83	.83	.80	.17	.11	.15	.15
	NATREG	.97	.03	.71	.75	.78	.81	.17	.07	.17	.16
	PDM	.53	.29	.04	.17	.12	.44	.35	.03	.10	.06
2/24	MAXPROBI	.80	.12	.29	0.0	.15	.82	.11	.27	0.0	.14
	MAXPROBII	.80	.12	.29	0.0	.15	.82	.11	.27	0.0	.14
	NATREG	.95	.05	.83	.68	.79	.74	.19	.23	.14	.18
	PDM $\lambda(96)$	.60	.33	.13	.19	.19	.54	.36	.03	.16	.09
	PDM $\lambda(98)$	.64	.27	.21	.21	.23	.54	.32	.05	.09	.07
	PDM λ'	.81	.11	.14	.44	.21	.81	.14	.14	0.0	.01
3W/24	MAXPROBI	.96	.03	.86	.81	.86	.70	.17	.35	.15	.30
	MAXPROBII	.96	.01	.87	.81	.87	.67	.18	.36	.15	.30
	NATREG	.94	.06	.86	.64	.81	.64	.26	.32	.16	.26
	PDM	.54	.20	.31	.16	.31	.44	.26	.14	.08	.13

TABLE V. CONT'D

Area/TAU	Method	DEPENDENT A0	DEPENDENT A1	DEPENDENT TS1	DEPENDENT TS2	DEPENDENT TS12	INDEPENDENT A0	INDEPENDENT A1	INDEPENDENT TS1	INDEPENDENT TS2	INDEPENDENT TS12
4/24	MAXPROBI	.85	.12	.04	.09	.09	.86	.12	.05	.07	.06
	MAXPROBII	.91	.07	.53	.54	.56	.80	.17	.07	.17	.16
	NATREG	.91	.09	.37	.42	.45	.81	.16	.04	.14	.13
	PDM	.57	.19	.05	.16	.10	.54	.22	.04	.11	.06
2/48	MAXPROBI	.79	.12	.27	.02	.15	.79	.12	.24	0.0	.14
	MAXPROBII	.97	.02	.89	.82	.86	.73	.18	.26	.11	.19
	NATREG	.86	.14	.52	.33	.45	.70	.23	.18	.09	.13
	PDM	.56	.34	.31	.19	.26	.37	.50	.04	.10	.09
3W/48	MAXPROBI	.93	.04	.82	.71	.80	.69	.18	.32	.11	.24
	MAXPROBII	.93	.04	.82	.74	.82	.66	.19	.33	.15	.28
	NATREG	.91	.09	.80	.52	.73	.62	.28	.27	.14	.22
	PDM	.48	.37	.21	.15	.21	.36	.42	.11	.11	.12
4/48	MAXPROBI	.97	.03	.79	.79	.80	.81	.15	.20	.16	.17
	MAXPROBII	.97	.03	.81	.82	.83	.77	.19	.16	.16	.17
	NATREG	.96	.04	.79	.73	.78	.80	.18	.19	.16	.17
	PDM	.37	.32	.04	.16	.10	.33	.36	.03	.09	.06

APPENDIX G

FIGURES

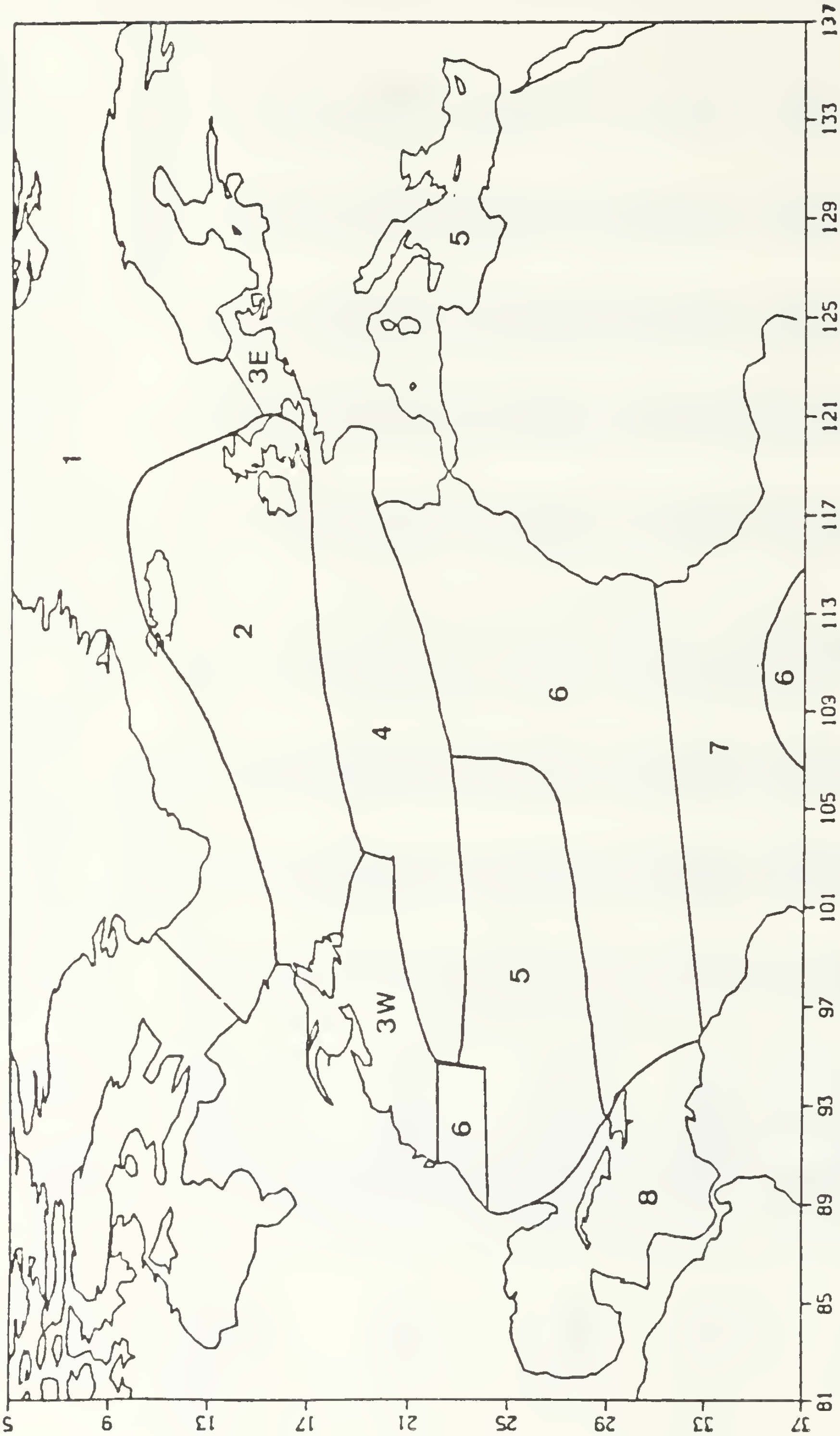

Fig. 1. Homogeneous areas for the North Atlantic Ocean, May, June and July, from Lowe (1984b).

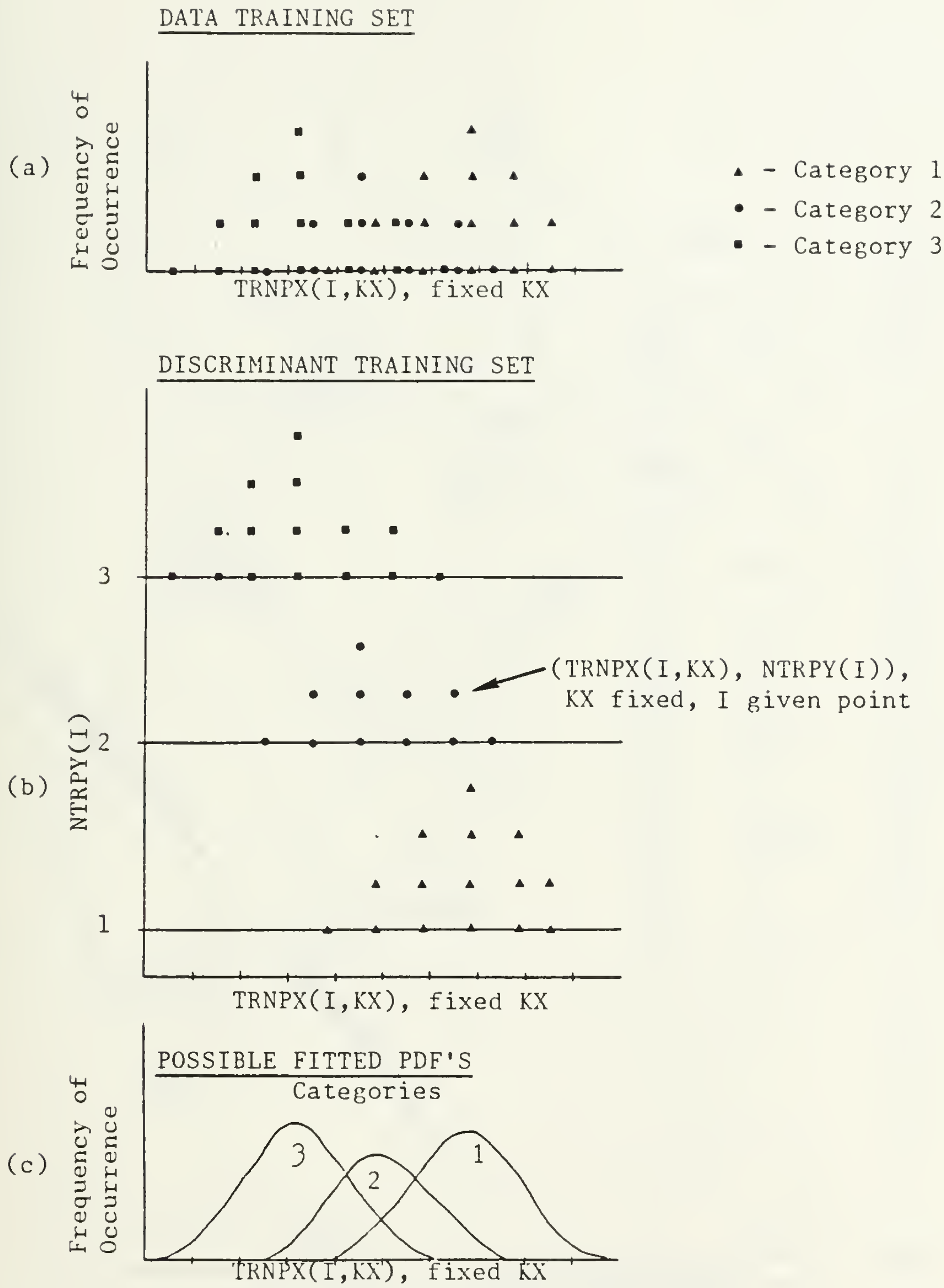

Fig. 2. Distribution diagrams for a sample training set where (a) shows the vertical stacking of observations; (b) shows the (a) data in their category discriminant sets; (c) shows the analytic representation of the data in (a).

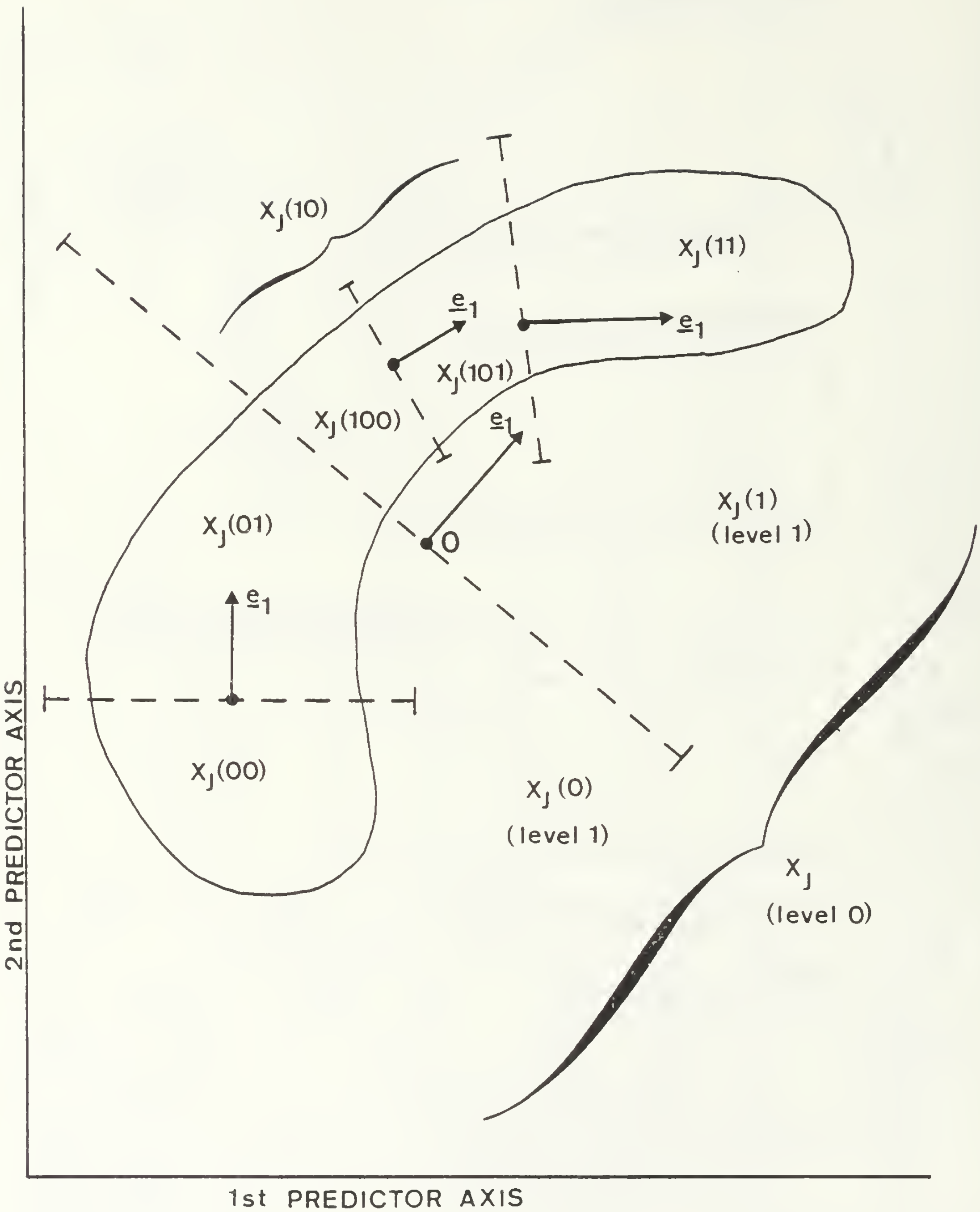

Fig. 3. A general representation of X_J in the case of two predictors, from Preisendorfer (1984).

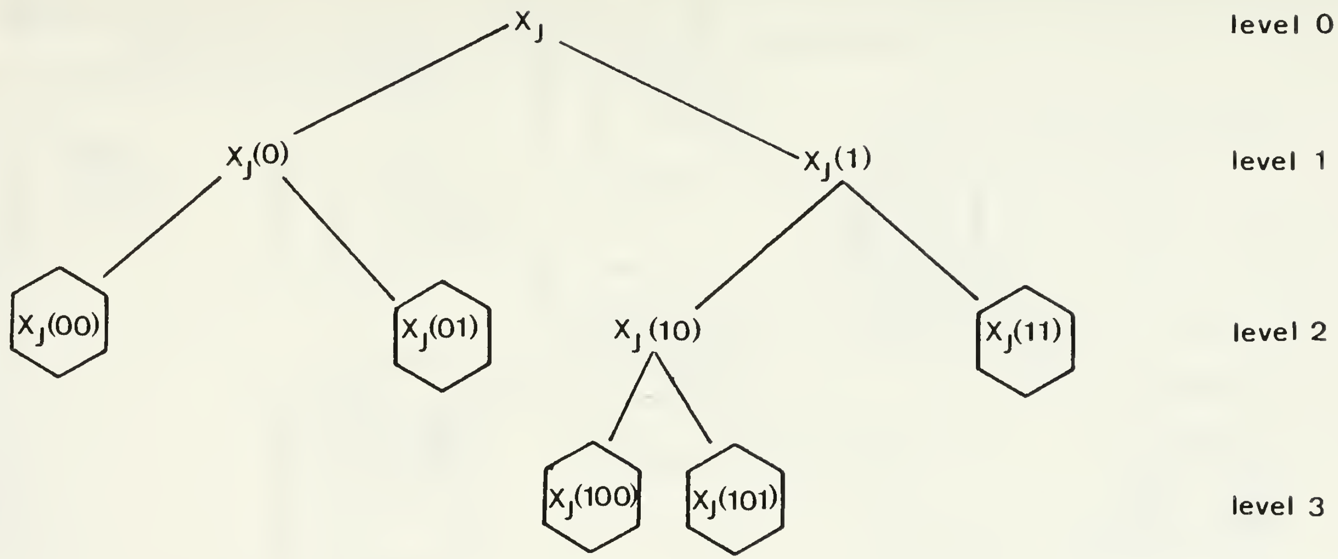

X_J is the inital category subset of the J^{th} category, $J=1,\ldots,Q$, located in E_K (space of K-dimensional predictors)

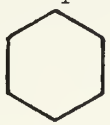 - denotes terminal nodes

Fig. 4. Schematic of the binary decomposition of a category subset, from Preisendorfer (1984).

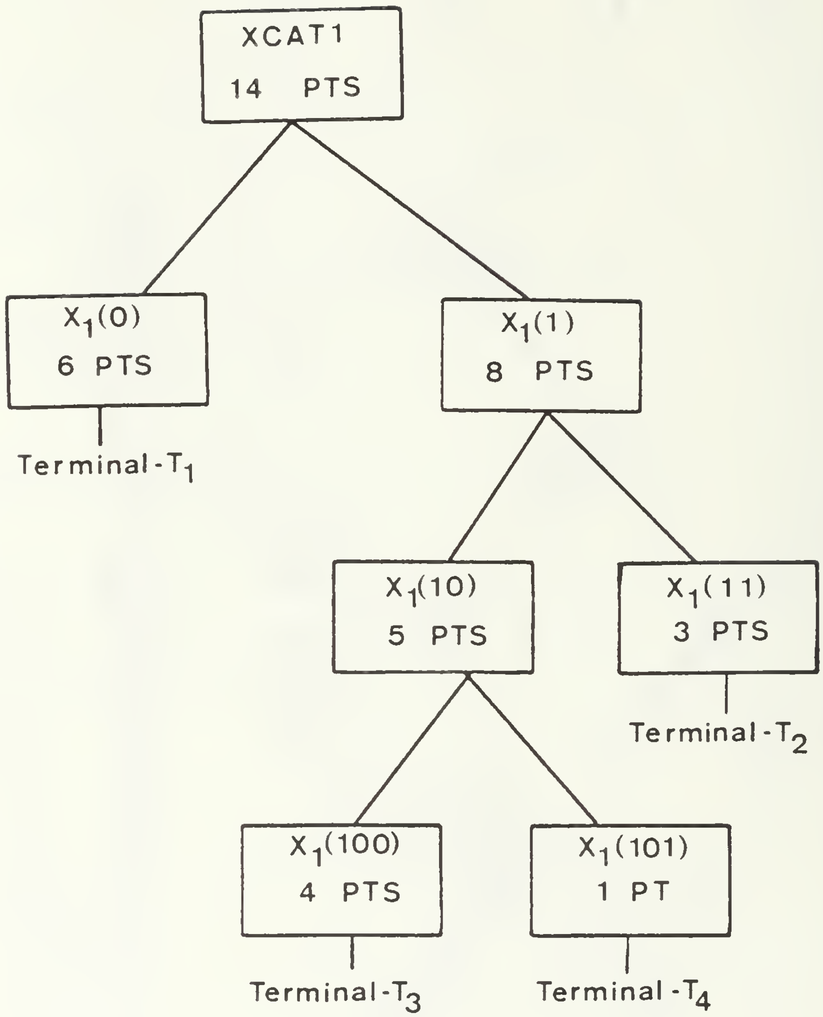

Fig. 5. Schematic of the binary decomposition of a sample set from area 2, TAU-24.

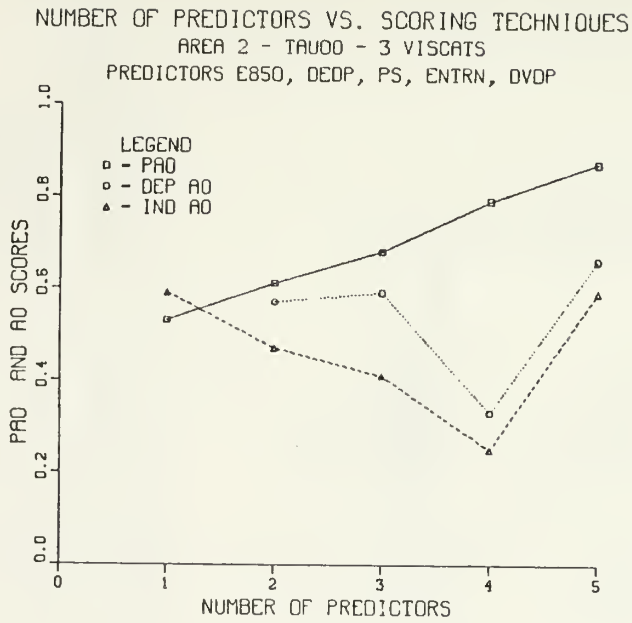

DEPENDENT DATA

FORECAST \ OBSERVED	1	2	3
3	36	67	1059
2	76	125	287
1	81	27	157

AO = 0.66
A1 = 0.27
TS1 = 0.21
TS2 = 0.21
TS12 = 0.24

INDEPENDENT DATA

FORECAST \ OBSERVED	1	2	3
3	42	64	538
2	17	17	177
1	8	6	83

AO = 0.59
A1 = 0.28
TS1 = 0.05
TS2 = 0.08
TS12 = 0.06

Fig. 6. Skill diagram and contingency table results for FATJUNE 1983, North Atlantic Ocean area 2, TAU-00, PDM model.

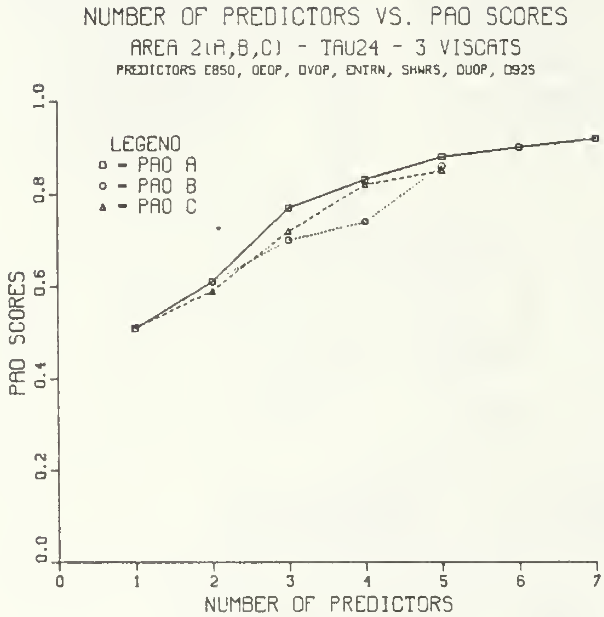

Fig. 7. Comparison of PAO scores for FATJUNE 1983, North Atlantic Ocean area 2(A,B,C), TAU-24, PDM model.

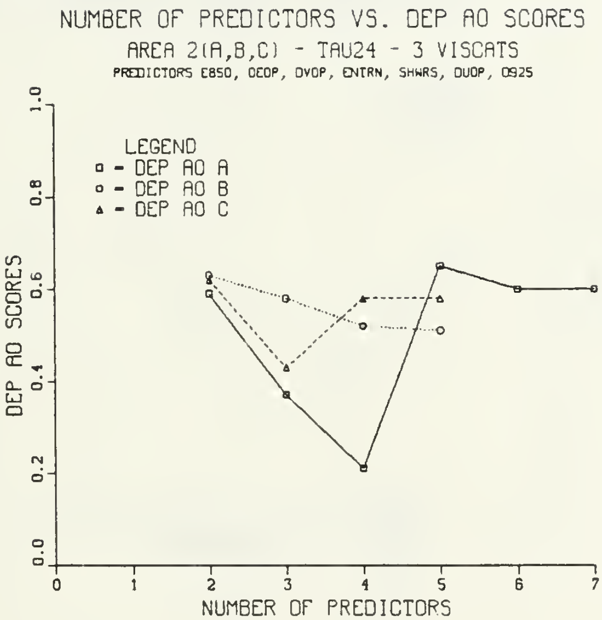

Fig. 8. Comparison of DEP AO scores for FATJUNE 1983, North Atlantic Ocean area 2(A,B,C), TAU-24, PDM model.

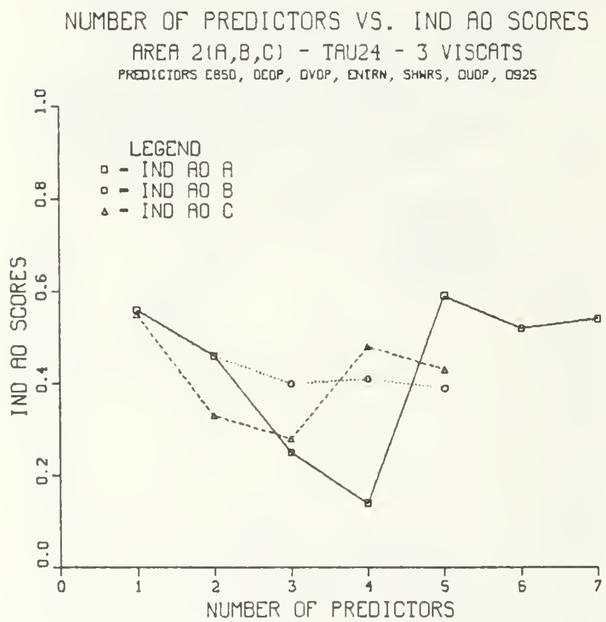

Fig. 9. Comparison of IND AO scores for FATJUNE 1983, North Atlantic Ocean area 2(A,B,C), TAU-24, PDM model.

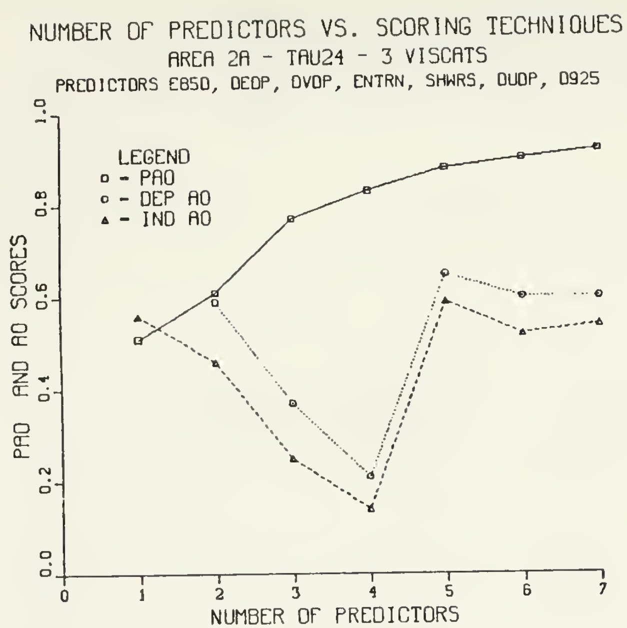

DEPENDENT DATA

FORECAST \ OBSERVED	1	2	3
3	37	57	870
2	89	130	404
1	35	11	88

AO = 0.60
A1 = 0.33
TS1 = 0.13
TS2 = 0.19
TS12 = 0.19

INDEPENDENT DATA

FORECAST \ OBSERVED	1	2	3
3	18	35	238
2	3	10	52
.	25	41	420

AO = 0.54
A1 = 0.36
TS1 = 0.03
TS2 = 0.16
TS12 = 0.09

Fig. 10. Skill diagram and contingency table results for FATJUNE 1983, North Atlantic Ocean area 2(A), TAU-24, PDM model.

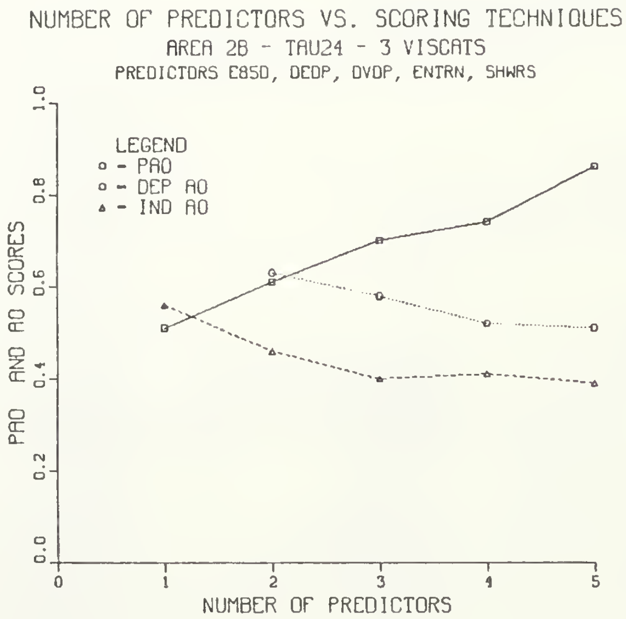

DEPENDENT DATA

FORECAST \ OBSERVED	1	2	3
3	23	42	691
2	87	143	536
1	46	11	107

AO = 0.51
A1 = 0.39
TS1 = 0.17
TS2 = 0.17
TS12 = 0.19

INDEPENDENT DATA

FORECAST \ OBSERVED	1	2	3
3	17	32	295
2	22	42	366
.	5	11	87

AO = 0.39
A1 = 0.49
TS1 = 0.04
TS2 = 0.09
TS12 = 0.08

Fig. 11. Skill diagram and contingency table results for FATJUNE 1983, North Atlantic Ocean area 2(B), TAU-24, PDM model.

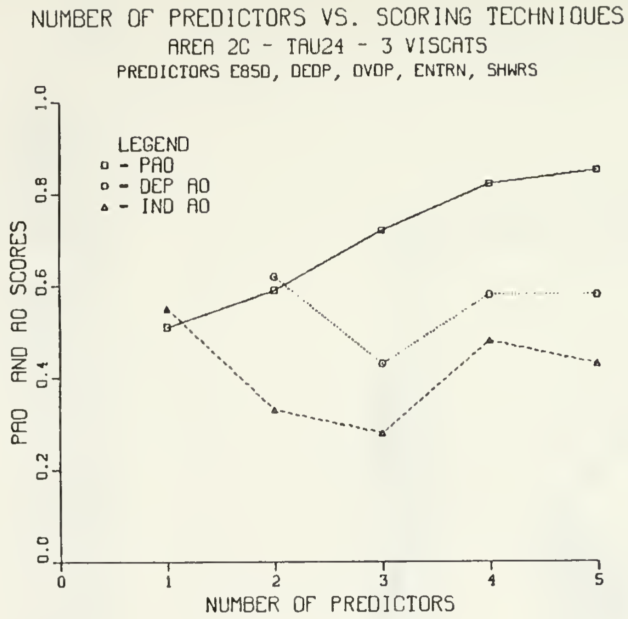

DEPENDENT DATA

FORECAST \ OBSERVED	1	2	3
3	20	45	766
2	10	86	274
1	141	67	314

AO = 0.58
A1 = 0.23
TS1 = 0.26
TS2 = 0.15
TS12 = 0.24

INDEPENDENT DATA

FORECAST \ OBSERVED	1	2	3
3	17	35	321
2	10	17	175
.	27	24	214

AO = 0.43
A1 = 0.29
TS1 = 0.09
TS2 = 0.07
TS12 = 0.08

Fig. 12. Skill diagram and contingency table results for FATJUNE 1983, North Atlantic Ocean area 2(C), TAU-24, PDM model.

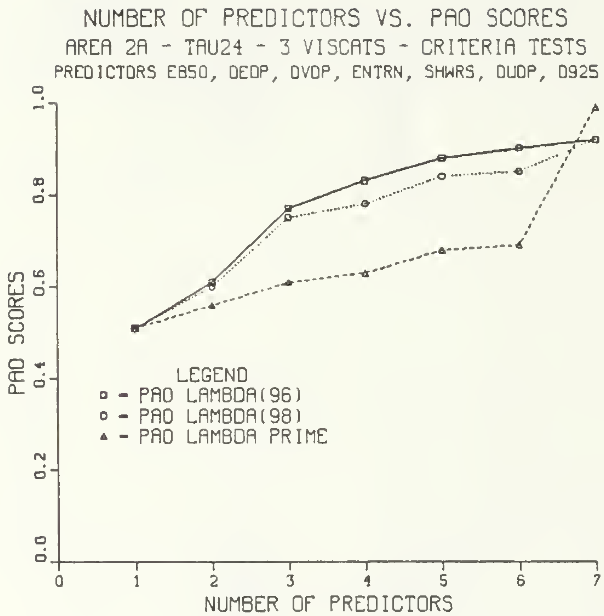

Fig. 13. Comparison of PAO scores for FATJUNE 1983, North Atlantic Ocean area 2(A), TAU-24, PDM model criteria tests.

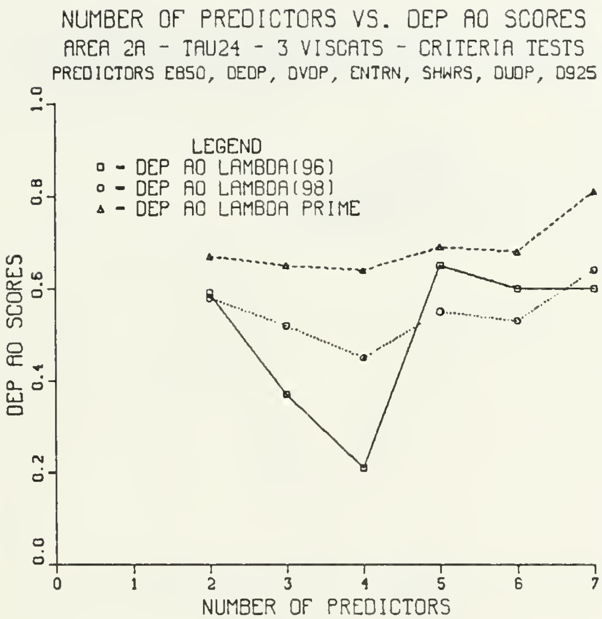

Fig. 14. Comparison of DEP AO scores for FATJUNE 1983, North Atlantic Ocean area 2(A), TAU-24, PDM model criteria tests.

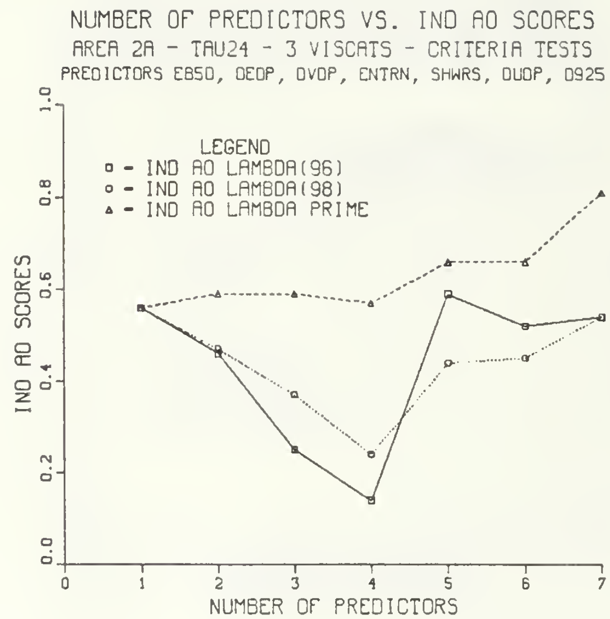

Fig. 15. Comparison of IND AO scores for FATJUNE 1983, North Atlantic Ocean area 2(A), TAU-24, PDM model criteria tests.

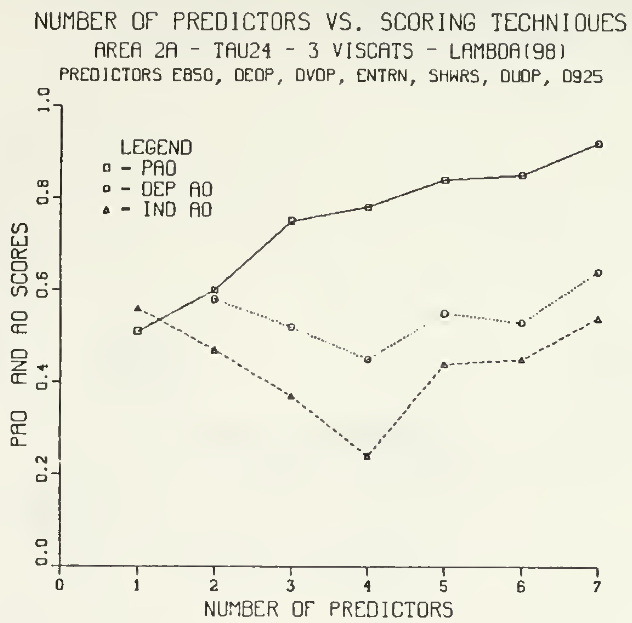

DEPENDENT DATA

FORECAST \ OBSERVED	1	2	3
3	42	54	916
2	58	126	327
1	61	18	119

AO = 0.64
A1 = 0.27
TS1 = 0.21
TS2 = 0.21
TS12 = 0.23

INDEPENDENT DATA

FORECAST \ OBSERVED	1	2	3
3	29	53	424
2	10	21	196
.	7	12	90

AO = 0.54
A1 = 0.32
TS1 = 0.05
TS2 = 0.09
TS12 = 0.07

Fig. 16. Skill diagram and contingency table results for FATJUNE 1983, North Atlantic Ocean area 2(A), TAU-24, PDM model lambda (98) criteria test.

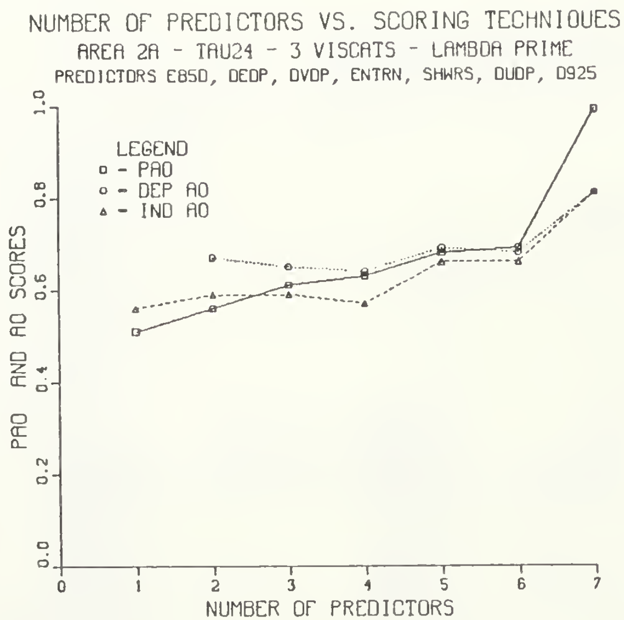

DEPENDENT DATA

FORECAST \ OBSERVED	1	2	3
3	131	132	1309
2	7	65	52
1	23	1	1

AO = 0.81
A1 = 0.11
TS1 = 0.14
TS2 = 0.44
TS12 = 0.21

INDEPENDENT DATA

FORECAST \ OBSERVED	1	2	3
3	43	86	683
2	1	0	27
.	2	0	0

AO = 0.81
A1 = 0.14
TS1 = 0.04
TS2 = 0.0
TS12 = 0.01

Fig. 17. Skill diagram and contingency table results for FATJUNE 1983, North Atlantic Ocean area 2(A), TAU-24, PDM model lambda prime criteria test.

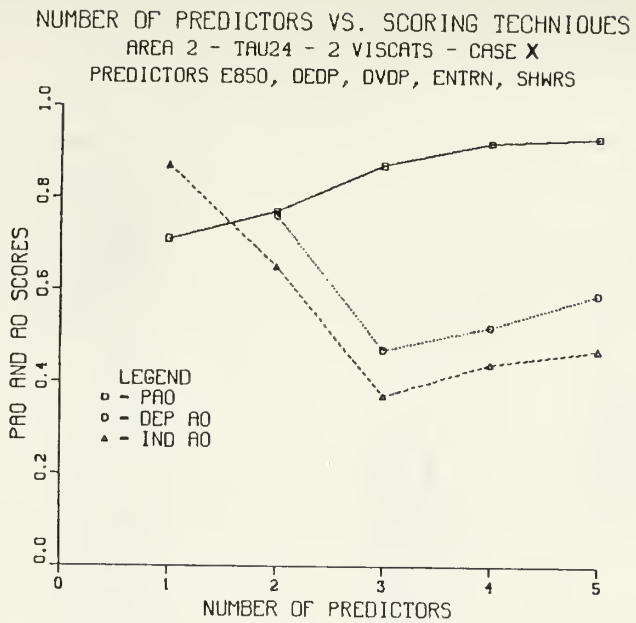

DEPENDENT DATA

FORECAST		OBSERVED 1	OBSERVED 2
	2	50	850
	1	164	657

AO = .59
A1 = .41
TS1=.19
TS2=.55

INDEPENDENT DATA

FORECAST		OBSERVED 1	OBSERVED 2
	2	31	357
	1	39	415

AO = .47
A1 = .53
TS1=.08
TS2=.44

Fig. 18. Skill diagram and contingency table results for FATJUNE 1983, North Atlantic Ocean area 2, TAU-24, Case X, PDM model.

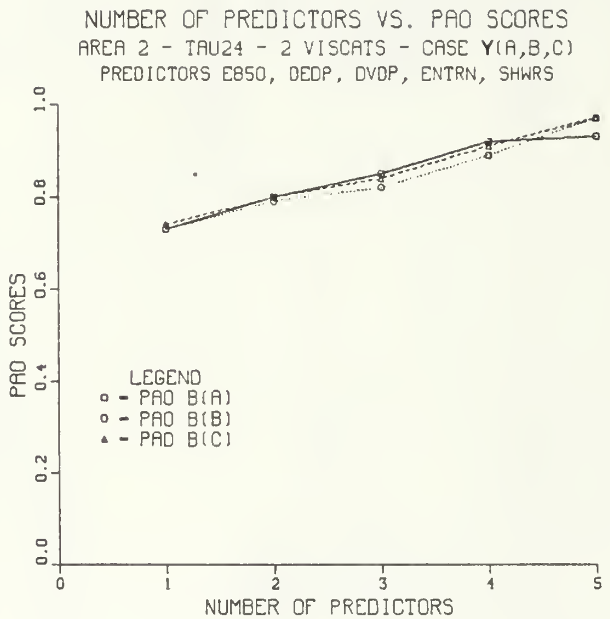

Fig. 19. Comparison of PAO scores for FATJUNE 1983, North Atlantic Ocean area 2, TAU-24, Case Y(A,B,C), PDM model.

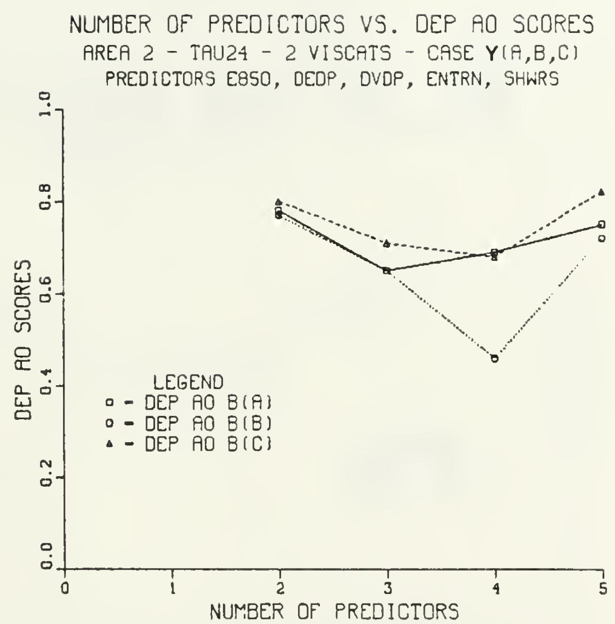

Fig. 20. Comparison of DEP AO scores for FATJUNE 1983, North Atlantic Ocean area 2, TAU-24, Case Y(A,B,C), PDM model.

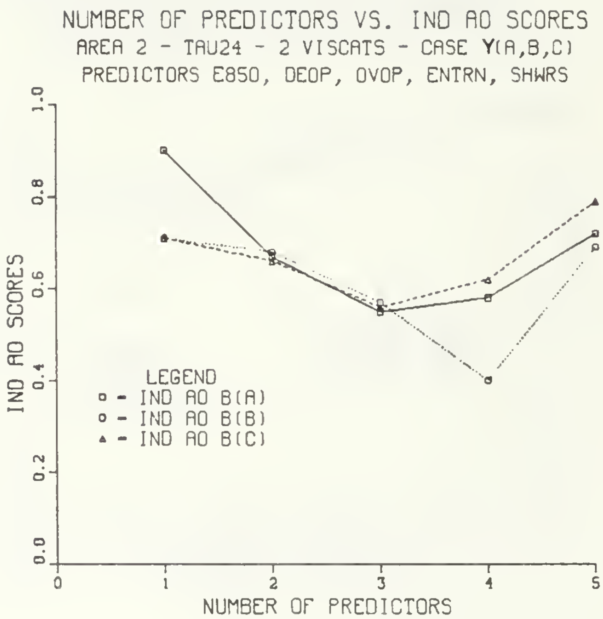

Fig. 21. Comparison of IND AO scores for FATJUNE 1983, North Atlantic Ocean area 2, TAU-24, Case Y(A,B,C), PDM model.

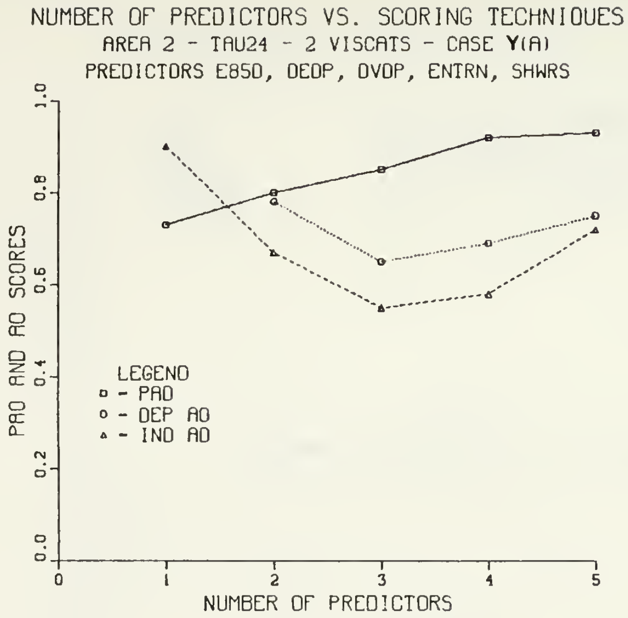

DEPENDENT DATA

FORECAST \ OBSERVED	1	2
2	98	1225
1	63	335

AO = .75
A1 = .25
TS1= .13
TS2= .74

INDEPENDENT DATA

FORECAST \ OBSERVED	1	2
2	30	587
1	16	209

AO = .72
A1 = .28
TS1= .06
TS2= .71

Fig. 22. Skill diagram and contingency table results for FATJUNE 1983, North Atlantic Ocean area 2, TAU-24 Case Y(A), PDM model.

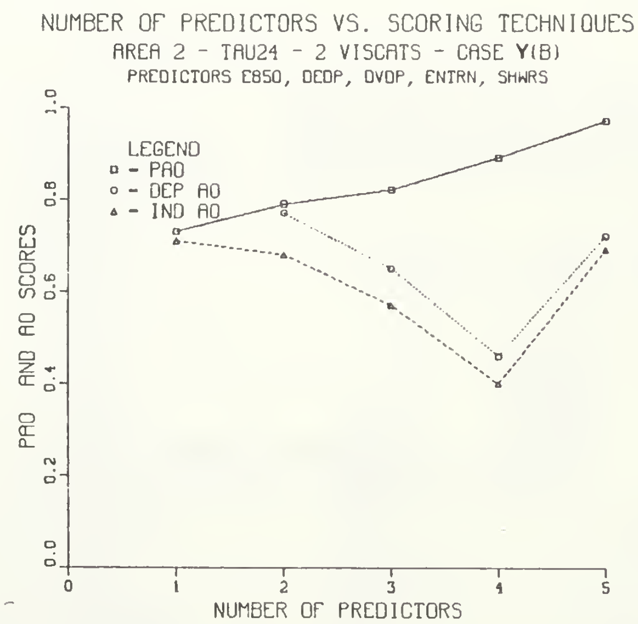

DEPENDENT DATA

FORECAST \ OBSERVED	1	2
2	85	1135
1	71	395

AO =.72
A1 =.28
TS1=.13
TS2=.70

INDEPENDENT DATA

FORECAST \ OBSERVED	1	2
2	31	592
1	13	241

AO =.69
A1 =.31
TS1=.05
TS2=.69

Fig. 23. Skill diagram and contingency table results for FATJUNE 1983, North Atlantic Ocean area 2, TAU-24 Case Y(B), PDM model.

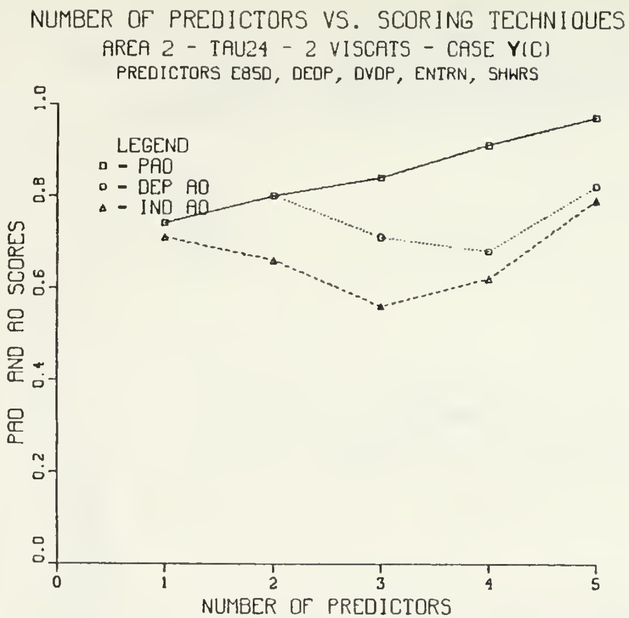

DEPENDENT DATA

FORECAST	OBSERVED 1	OBSERVED 2
2	76	1299
1	79	228

AO = .82
A1 = .18
TS1 = .21
TS2 = .81

INDEPENDENT DATA

FORECAST	OBSERVED 1	OBSERVED 2
2	34	685
1	9	153

AO = .79
A1 = .21
TS1 = .05
TS2 = .79

Fig. 24. Skill diagram and contingency table results for FATJUNE 1983, North Atlantic Ocean area 2, TAU-24 Case Y(C), PDM model.

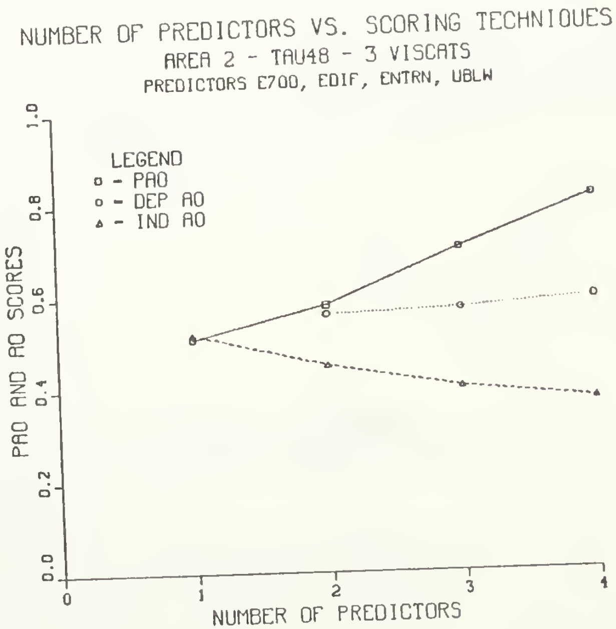

DEPENDENT DATA

FORECAST \ OBSERVED	1	2	3	
3	19	34	820	AO = 0.59
2	57	164	506	A1 = 0.34
1	103	28	127	TS1 = 0.31
				TS2 = 0.19
				TS12 = 0.26

INDEPENDENT DATA

FORECAST \ OBSERVED	1	2	3	
3	18	29	285	AO = 0.37
2	18	48	398	A1 = 0.50
.	6	10	107	TS1 = 0.4
				TS2 = 0.10
				TS12 = 0.09

Fig. 25. Skill diagram and contingency table results for FATJUNE 1983, North Atlantic Ocean area 2, TAU-48, PDM model.

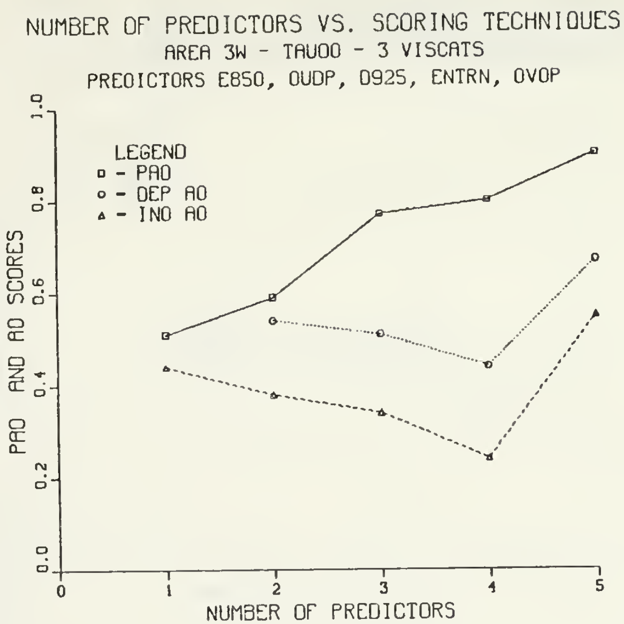

DEPENDENT DATA

FORECAST \ OBSERVED	1	2	3
3	126	94	843
2	54	73	129
1	110	22	81

AO = 0.67
A1 = 0.20
TS1 = 0.28
TS2 = 0.19
TS12 = 0.27

INDEPENDENT DATA

FORECAST \ OBSERVED	1	2	3
3	82	76	385
2	13	10	84
1	23	16	67

AO = 0.55
A1 = 0.25
TS1 = 0.11
TS2 = 0.07
TS12 = 0.09

Fig. 26. Skill diagram and contingency table results for FATJUNE 1983, North Atlantic Ocean area 3W, TAU-00, PDM model.

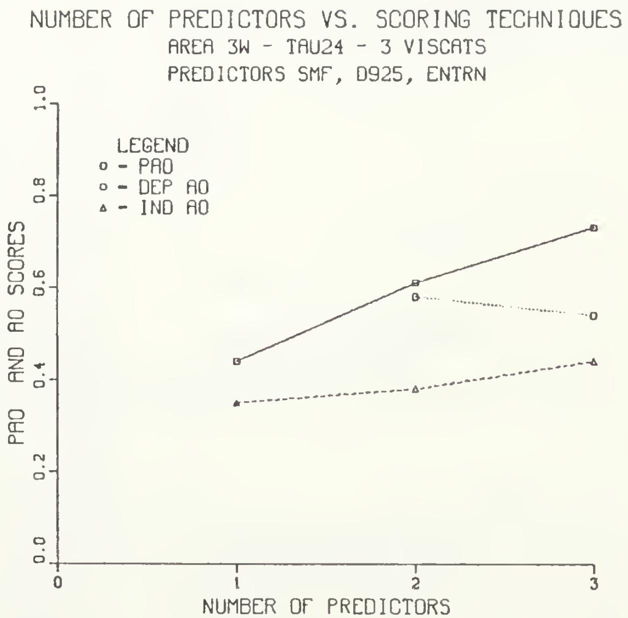

DEPENDENT DATA

FORECAST \ OBSERVED	1	2	3	
3	46	37	473	AO = 0.54
2	26	82	156	A1 = 0.20
1	197	53	314	TS1 = 0.31
				TS2 = 0.16
				TS12 = 0.31

INDEPENDENT DATA

FORECAST \ OBSERVED	1	2	3	
3	30	38	240	AO = 0.44
2	14	16	90	A1 = 0.26
.	42	34	179	TS1 = 0.14
				TS2 = 0.08
				TS12 = 0.13

Fig. 27. Skill diagram and contingency table results for FATJUNE 1983, North Atlantic Ocean area 3W, TAU-24, PDM model.

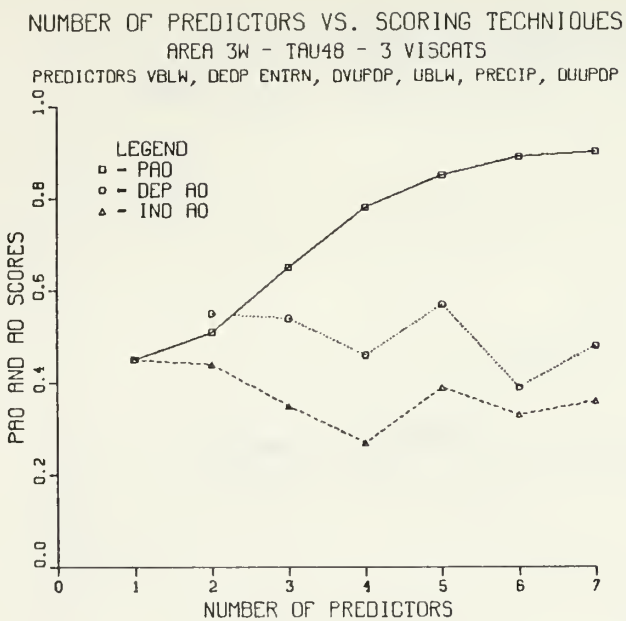

DEPENDENT DATA

FORECAST	OBSERVED 1	OBSERVED 2	OBSERVED 3
3	68	57	511
2	112	102	353
1	100	32	156

AO = 0.48
A1 = 0.37
TS1 = 0.21
TS2 = 0.15
TS12 = 0.21

INDEPENDENT DATA

FORECAST	OBSERVED 1	OBSERVED 2	OBSERVED 3
3	50	44	205
2	33	36	216
.	26	18	111

AO = 0.36
A1 = 0.42
TS1 = 0.11
TS2 = 0.11
TS12 = 0.12

Fig. 28. Skill diagram and contingency table results for FATJUNE 1983, North Atlantic Ocean area 3W, TAU-48, PDM model.

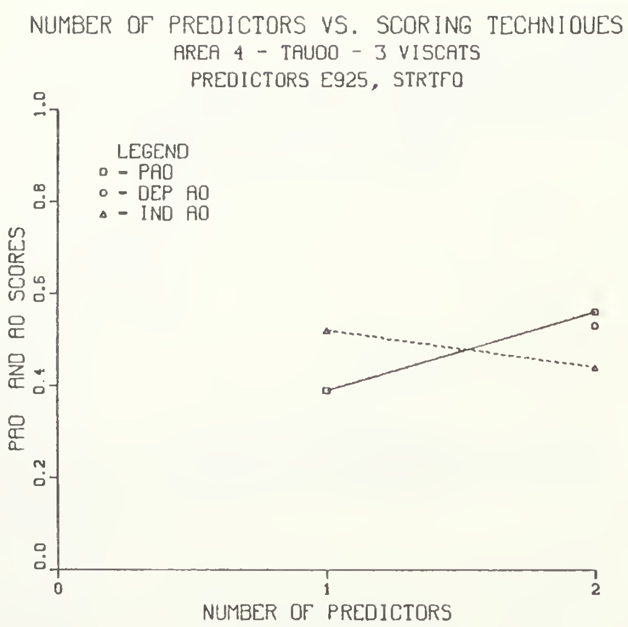

DEPENDENT DATA

FORECAST \ OBSERVED	1	2	3
3	19	102	1469
2	31	180	687
1	32	112	542

AO = 0.53
A1 = 0.29
TS1 = 0.04
TS2 = 0.17
TS12 = 0.12

INDEPENDENT DATA

FORECAST \ OBSERVED	1	2	3
3	9	92	639
2	6	51	414
.	11	54	321

AO = 0.44
A1 = 0.35
TS1 = 0.03
TS2 = 0.10
TS12 = 0.06

Fig. 29. Skill diagram and contingency table results for FATJUNE 1983, North Atlantic Ocean area 4, TAU-00, PDM model.

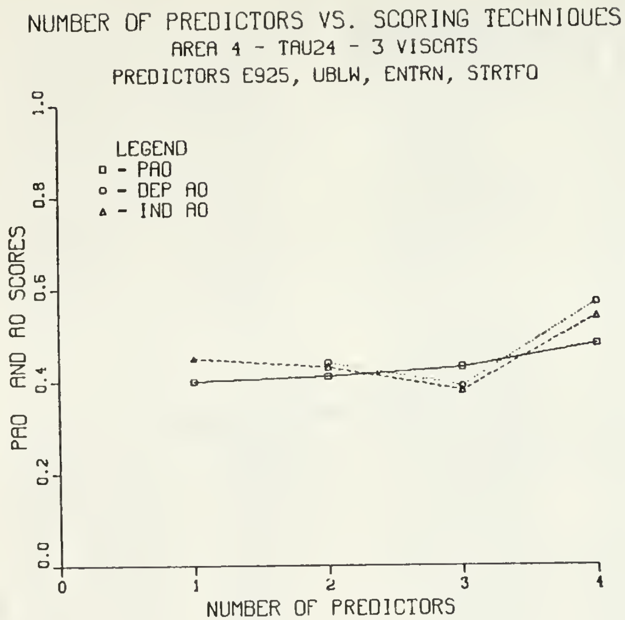

DEPENDENT DATA

FORECAST \ OBSERVED	1	2	3
3	20	148	1486
2	8	87	259
1	46	129	669

AO = 0.57
A1 = 0.19
TS1 = 0.05
TS2 = 0.16
TS12 = 0.10

INDEPENDENT DATA

FORECAST \ OBSERVED	1	2	3
3	16	43	327
2	2	27	166
.	16	43	327

AO = 0.54
A1 = 0.22
TS1 = 0.04
TS2 = 0.11
TS12 = 0.06

Fig. 30. Skill diagram and contingency table results for FATJUNE 1983, North Atlantic Ocean area 4, TAU-24, PDM model.

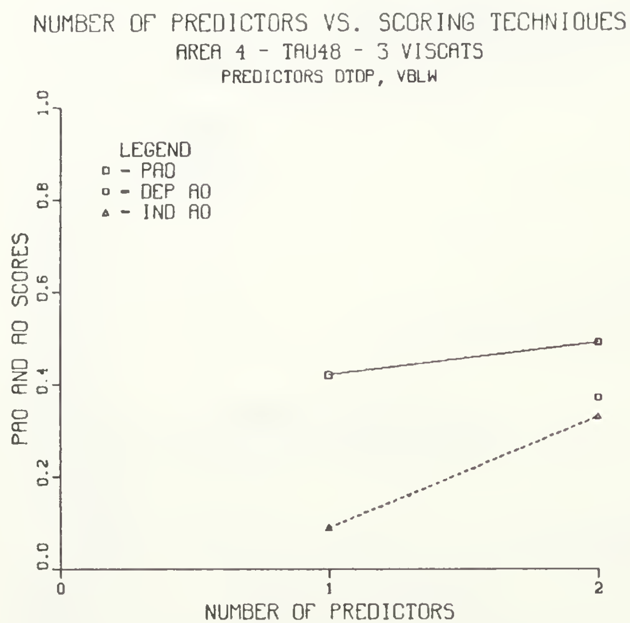

DEPENDENT DATA

FORECAST	OBSERVED 1	OBSERVED 2	OBSERVED 3
3	35	139	902
2	15	174	725
1	49	97	911

AO = 0.37
A1 = 0.32
TS1 = 0.04
TS2 = 0.16
TS12 = 0.10

INDEPENDENT DATA

FORECAST	OBSERVED 1	OBSERVED 2	OBSERVED 3
3	7	60	446
2	4	53	421
1	14	70	461

AO = 0.33
A1 = 0.36
TS1 = 0.03
TS2 = 0.09
TS12 = 0.06

Fig. 31. Skill diagram and contingency table results for FATJUNE 1983, North Atlantic Ocean area 4, TAU-48, PDM model.

LIST OF REFERENCES

Aldinger, W.T., 1979: Experiments on Estimating Open Ocean Visibilities Using Model Output Statistics. M.S. Thesis (R.J. Renard, advisor), Dept. of Meteorology, Naval Postgraduate School, Monterey, CA, 81 pp.

Best, D.L., and Pryor, S.P., 1983: Air Weather Service Model Output Statistics System Project Report. AFGWC/Pr-83/001, United States Air Force Air Weather Service (MAC), Air Force Global Weather Central, Offutt AFB, NE, 85 pp.

Diunizio, M., 1984a: An Evaluation of Discretized Conditional Probability and Linear Regression Threshold Techniques in Model Output Statistics Forecasting of Visibility Over the North Atlantic Ocean. M.S. Thesis (R.J. Renard, advisor), Dept. of Meteorology, Naval Postgraduate School, Monterey, CA, 233 pp.

________, 1984b: An Evaluation of Statistical Significance Associated with the Results of My September 1984 Thesis Based Upon the Null Hypothesis and Associated 95% Confidence Interval, unpublished manuscript, Dept. of Meteorology, Naval Postgraduate School, Monterey, CA, 22 pp.

Department of the Navy, 1979: CV NATOPS Manual, Office of the Chief of Naval Operations, Washington, DC, 156 pp.

Karl, M.L., 1984: Experiments in Forecasting Atmospheric Marine Horizontal Visibility Using Model Output Statistics with Conditional Probabilities of Discretized Parameters. M.S. Thesis (R.J. Renard, advisor), Dept. of Meteorology, Naval Postgraduate School, Monterey, CA, 165 pp.

Koziara, M.C., R.J. Renard and W.J. Thompson, 1983: Estimating Marine Fog Probability Using a Model Output Statistics Scheme. Monthly Weather Review. 111, p2333-2340.

Lowe, P., 1984a: The Use of Decision Theory for Determining Thresholds for Categorical Forecasts, unpublished manuscript, Naval Environmental Prediction Research Facility, Monterey, CA, 20 pp.

________, 1984b: The Use of Multi-Variate Statistics for Defining Homogeneous Atmospheric Regions Over the North Atlantic Ocean, unpublished manuscript, Naval Environmental Prediction Research Facility, Monterey, CA, 15 pp.

Preisendorfer, R.W., 1983a: Proposed Studies of Some Basic Marine Atmospheric Visibility Prediction Schemes Using Model Output Statistics, unpublished manuscript, Department of Meteorology, Naval Postgraduate School, Monterey, CA, 28 pp.

________, 1983b: Maximum-Probability and Natural Regression Prediction Strategies, unpublished manuscript, Department of Meteorology, Monterey, CA, 10 pp.

, 1983c: Tests for Functional Dependence of Predictors, unpublished manuscript, Department of Meteorology, Naval Postgraduate School, Monterey, CA, 5 pp.

, 1984: The Principal Discriminant Method of Prediction, unpublished manuscript, PMEL, Seattle, WA, 25 pp.

Renard, R.J. and W.T. Thompson, 1984: Estimating Visibility Over the North Pacific Ocean Using Model Output Statistics. National Weather Digest. 9, p18-25.

Selsor, H.D., 1980: Further Experiments Using a Model Output Statistics Method in Estimating Open Ocean Visibility. M.S. Thesis (R.J. Renard, advisor), Dept. of Meteorology, Naval Postgraduate School, Monterey, CA, 121 pp.

University of California, 1983: BMDP Statistical Software, 1983 Edition, Department of Biomathematics, University of California at Los Angeles, University of California Press, 726 pp.

Wooster, M.H., 1984: An Evaluation of Discretized Conditional Probability and Linear Regression Threshold Techniques in Model Output Statistics Forecasting of Cloud Amount and Ceiling Over the North Atlantic Ocean. M.S. Thesis (R.J. Renard, advisor), Dept. of Meteorology, Naval Postgraduate School, Monterey, CA, 187 pp.

Yavorsky, P.G., 1980: Experiments Concerning Categorical Forecasts of Open-Ocean Visibility using Model Output Statistics. M.S. Thesis (R.J. Renard, advisor), Dept. of Meteorology, Naval Postgraduate School, Monterey, CA, 87 pp.

INITIAL DISTRIBUTION LIST

		No. Copies
1.	Defense Technical Information Center Cameron Station Alexandria, VA 22314	2
2.	Library, Code 0142 Naval Postgraduate School Monterey, CA 93943	2
3.	Meteorology Reference Center, Code 63 Department of Meteorology Naval Postgraduate School Monterey, CA 93943	1
4.	Professor Robert J. Renard, Code 63Rd Chairman, Department of Meteorology Naval Postgraduate School Monterey, CA 93943	6
5.	Chairman (Code 68Mr) Department of Oceanography Naval Postgraduate School Monterey, CA 93943	1
6.	Dr. Rudolph W. Preisendorfer NOAA/PMEL/R/E/PM Bin C15700 Bldg. 3 7600 Sand Point Way, N.E. Seattle, WA 98115-0070	2
7.	Mr. Paul Lowe Naval Environmental Prediction Research Facility Monterey, CA 93940	1
8.	Dr. Robert Godfrey Naval Environmental Prediction Research Facility Monterey, CA 93940	1
9.	Director Naval Oceanography Division Naval Observatory 34th and Massachusetts Avenue NW Washington, D.C. 20390	1

10. Commander 1
Naval Oceanography Command
NSTL Station
Bay St. Louis, MS 39522

11. Commanding Officer 1
Naval Oceanographic Office
NSTL Station
Bay St. Louis, MS 39522

12. Commanding Officer 1
Fleet Numerical Oceanography Center
Monterey, CA 93940

13. Commanding Officer 1
Naval Ocean Research and
Development Activity
NSTL Station
Bay St. Louis, MS 39522

14. Commanding Officer 1
Naval Environmental Prediction
Research Facility
Monterey, CA 93940

15. Chairman, Oceanography Department 1
U.S. Naval Academy
Annapolis, MD 21402

16. Chief of Naval Research 1
800 N. Quincy Street
Arlington, VA 22217

17. Office of Naval Research (Code 480) 1
Naval Ocean Research and Development
Activity
NSTL Station
Bay St. Louis, MS 39522

18. Commander (Air-370) 1
Naval Air Systems Command
Washington, D.C. 20360

19. Chief, Ocean Services Division 1
National Oceanic and Atmospheric
Administration
8060 Thirteenth Street
Silver Spring, MD 20910

20. Dr. Alan Weinstein 1
Leader, Code 422
Ocean Sciences Division
Office of Naval Research
Arlington, VA 22217

21. Mr. Gil Ross, Met 09 1
Meteorological Office
Bracknell, Berkshire
England

22. Chief, Technical Procedures Branch 1
Meteorological Services Division
National Oceanic and Atmospheric
Administration
National Weather Service
Silver Spring, MD 20910

23. Chief, Technical Services Division 1
United States Air Force
Air Weather Service (MAC)
Air Force Global Weather Central
Offutt AFB, NB 68113

24. LCDR Kristine C. Elias 1
43 Cielo Vista Drive
Monterey, CA 93940

2̣1221

Thesis
E3157 Elias
c.1 Forecasting atmospheric visibility over the summer North Atlantic using the Principal Discriminant Method.